STORM SURGE ATTENUATION

KASPER DE VAAN
UTRECHT UNIVERSITY, FACULTY OF GEOSCIENCES

Building with nature applied for the Western Scheldt

Modelling storm surge attenuation by a double dike system

Kasper de Vaan – 6576478

In partial fulfilment of the requirements for the degree of Master of Science in Marine Sciences
At Utrecht University, Faculty of Geosciences

Supervisors:

MSc. Jim van Belzen
Prof. Dr. Tjeerd Bouma

Date: 30 January 2020

Course code: GEO4-1520 MSc Thesis
Credits: 30 ECTS

Abstract

The world's largest deltas are starved in sediment while the sea level keeps rising. Hundreds of millions of people become more vulnerable to flooding's by the end of this century. The urge to rethink the current coastal protection system is larger than it has ever been. Ecological based coastal engineering has the potential to provide an answer to the problem as can offer long-term sustainability and resilience, a double dike system is an application of building with nature. The goal of this research is to understand if a double dike system could attenuate a storm surge wave in an estuary. The Western Scheldt estuary is used as a test case. A conceptual model in Python is developed, dividing the estuary in three sections, water flow is calculated with the equations of Chezy. Selecting the friction as calibration parameter, the model is calibrated based on measurements from Rammegors and Perkpolder. The model is validated using another period from the two polders, selecting the appropriate calibration parameter based statistical tests. Results show that adding polders increases the attenuation capacity, adding larger polder results in a higher attenuation capacity. All the polders have an optimal inlet area at which the attenuation capacity is maximal. A large scale implemented double dike system can reduce the maximal water level in the Western Scheldt during a storm surge by 11%. This research has provided a first insight in the potential of the attenuation capacity of double dike system which can be applied in estuaries worldwide.

Contents

List of Figures

List of tables

List of abbreviations

CRT	Control Reduced Tide
FCA	Flood controlled area
IoA	Index of Agreement
MHW	Mean high water
MLW	Mean low water
MWL	Mean water level
NAP	Nieuw Amsterdams Peil (Dutch water standard)
RSME	Root Means Square Error
WS	Western Scheldt

Introduction

The world's densely populated deltas like the Mekong, Ganges Brahmaputra, Mississippi and Yangtze are struggling to protect the land from the rising sea level (Blum & Roberts, 2009; C. Schmidt, 2015; C. W. Schmidt, 2015; Yang et al., 2017). Their situation may become even more vulnerable in the next century. The RCP8.5 scenario predicts a sea level rise of 0.98m by 2100 (Pörtner et al., 2019), putting hundreds of millions of people in risk of flooding (Nicholls et al., 2007). As many large cities are located along the coast, 13% of the world's urban population will be affected (McGranahan, Balk, & Anderson, 2007). The financial burden due to flood damages is estimated at $1 trillion per year from 2050 on if we do not act (Hallegatte, Green, Nicholls, & Corfee-Morlot, 2013). To protect all the people and assets in the future it is necessary to change the coastal defence management. The fast rise in sea level requires a flexible and relatively cheap solution which can be applied on a large scale. The urge to rethink the coastal management strategy is larger than it has ever been. Building with nature provides long-term sustainable and resilient solutions while being cost-effective. This method strives to use the natural defence capacity of a system instead of hard engineering (e.g. dikes) (Vriend & Koningsveld, 2012). Current hard engineering reduces the dynamics of a natural system (van Wesenbeeck et al., 2014; Yang et al., 2017), while a nature based solution makes use of these dynamics and thereby strengthen the system as a whole. The current hard engineering will be unmaintainable during the next centuries. The need to revise the coastal defence is unavoidable. Being able to apply the building with nature concept on a large scale gives the opportunity to save guard the future of hundreds of millions of lives and protect the worlds ecosystems. Ecological engineering is now viewed by most as the best method to provide a long-term sustainable and resilient coastal defence (Borsje et al., 2011; Bouma et al., 2014; Hinkel et al., 2014; Kabat et al., 2009; Temmerman et al., 2013; Van Slobbe et al., 2013). An open research gap is the attenuation capacity of these systems during a storm surge (Bouma et al., 2014; Morris, Konlechner, Ghisalberti, & Swearer, 2018). In this research is explored what the possibilities are for a double dike system as coastal defence in a delta system. This is achieved by modelling a double dike system to understand how this may attenuate a storm surge wave.

Ecological engineering has been applied on small scales in different locations worldwide, examples range from restoration and conservation of mangrove forests and oyster reefs to the creation of salt marshes. Making use of the natural capacity to attenuate waves or enhance sedimentation results in a safer coastal zone (Cheong et al., 2013; Horstman et al., 2014; Jones, Hole, & Zavaleta, 2012; Möller et al., 2014; Narayan et al., 2016; Shepard, Crain, & Beck, 2011). In the United states, observations has shown wave attenuation of mangrove wetlands during hurricanes is up to 25 cm/km (Krauss et al., 2009; Jeroen Stark, Plancke, Ides, Meire, & Temmerman, 2016; J Stark, Van Oyen, Meire, & Temmerman, 2015), thereby reducing the risk of flooding of the hinterland. The best-known example may well be the sand motor in front of the Dutch coast, which has increased the coastal safety while being cheaper to implement than yearly sand nourishments (Brière, Janssen, Oost, Taal, & Tonnon, 2018).

The south west delta of the Netherlands is used as a test case for exploring the possibilities for building with nature, this estuary is extremely well monitored. Since a catastrophic flood in 1953, were more than 1800 lives were lost, has the Dutch government been highly motivated to protect the land from the sea. After this flooding, plans were made for the construction of the Delta infrastructure to protect the land against future flooding's. At the moment is the Scheldt delta mainly protected by hard measures. The current Delta standard prescribes that the risk of flooding must be smaller than once in 10000 years (Kabat et al., 2009; Sterl, van den Brink, Haarsma, de Vries, & van Meijgaard, 2009). The increased safety however, comes at a cost, the maintenance of the Delta infrastructure is €1.6 billion per year until 2050 (Kabat et al., 2009). Despite these investments, the long-term effectiveness and sustainability of these constructions is increasingly questioned. As they causes problems like are salt intrusion (Nguyen, 2008) and ecological issues like eutrophication, habitat loss, pollution and stratification (van Wesenbeeck et al., 2014). Also, soil compaction (Temmerman & Kirwan, 2015; Temmerman et al., 2013) and sediment starvation (Ofori, van der Wegen, Roelvink, & de Ronde, 2019; Tangelder, Troost, van den Ende, & Ysebaert, 2012). Combine this with a rising sea level, and the net effect is a relative sea level rise of 0.65 – 1.30 meters for The Netherlands by 2100 (Kabat et al., 2009). Further, stronger future storm are precited in the North Sea (Debernard & Røed, 2008; Donat et al., 2011; Weisse, von Storch, Niemeyer, & Knaack, 2012). Realize that the largest part of Zeeland is located below sea level and the urge to rethink the coastal management strategy becomes evident.

To be able to protect the Southern part of the Dutch coast the project Zeeland 2121 is started, in which more sustainable coastal defence options are researched. The scenarios consist of dike heightening, dike widening, move the dike land inwards and create a double dike system. The last option is the most interesting as we can use the already existing dikes, thereby is it the cheapest solution to implement (Dubbeldam, 2019). A double dike system brings beside flood safety benefits to the area: wet agriculture, energy production and increased tourism. This solution consists of creating inlets in the polders, so that water can enter the polder. The old inland sea dike will function as the final barrier between the sea and the land, hence small dike heightening will be necessary to ensure the Delta safety standards. During a storms surge water will enter the polder, thereby reducing the water level in Western Scheldt. The goal of this research is to investigate with a model how this system will function during a storm surge and if it is able to dampen the surge for the whole estuary.

The conceptual model developed is validated with measured data to test whether it reflects actual water flow. The model simulations provide insight how the polder and inlet design influence the attenuation capacity. From these results is determined which design leads to the highest attenuation capacity and what the attenuation capacity is.

Can a storm surge wave be attenuated by a double dike system in the Western Scheldt?
Before starting with the research I defined what attenuation capacity is, below you find the definitions from the dictionary (Oxford English Dictionary, 2019). To rephrase it for this research: the ability of the double dike system to reduce the maximal water level in the Western Scheldt during a storm surge, expressed as a percentage.

Attenuation, n. - *The process of weakening, as if by dilution*
Capacity, n. - *Ability to receive or contain; holding power. Obsolete (in general sense).*

Research Questions

- Can a storm surge wave be attenuated by a double dike system in the Western Scheldt?
  - How to predict the water level in the polder?
  - How to model a storm surge?
  - Can the model be validated with data from field measurements?
  - How does the design of the double dike infleunce the attenuation capacity?
  - Can a simple ratio be used to estimate the attenuation capacity?

Approach

Before developing the model in Python, the research is started with a simplified volume based (back of the envelope) calculation. The aim was to get a first insight the potential of the double dike system for the Western Scheldt. Next was the model developed, in the model are the polders and estuary represented as volumes. The model should work on hourly to daily timescale, similar to the time scale of most storms. A 1-minute frequency is used, an hourly time scale is too coarse, and a 1-second time step would require unnecessary computational power and time. The model is divided in three sections, to include spatial variability in the estuary. There is no interaction between the sections and the estuary water levels are uniform within one section. The sections are 20 kilometres long, a bias in the estuary water volume calculation is therefore inevitable. The estuary water volume data is therefore checked with values found in previous research.

The water flow is calculated by a water balance. The water balance consists of the semidiurnal tidal-wave (Huthnance, 1991) and a storm surge. Outflow from the polders is restricted, the measure of restriction is determined by the area of the inlet in the dike (e.g. friction). The water inflow has the same restrictions, both flow restrictions will be modelled by the Chezy equation with a corresponding roughness length for a concrete inlet. The choice to use the Chezy equations for the discharge calculations, came with two assumptions. First, the roughness length is constant over the full length of the inlet area. This assumption is justified as this is only a relative short concrete surface (20 m) and concrete is a rigid surface with a constant roughness length (Morvan, Knight, Wright, Tang, & Crossley, 2008). Secondly, the flow velocity calculated is flow averaged velocity. In practise is the flow velocity through the inlet slower near the walls and bottom while the highest flow velocity is achieved in the middle. However, the discharge is the main interest for this model, a flow averaged velocity is sufficient to calculate the discharge.
Two types of dikes are present in the model. The dike between the polders and the estuary is called primary dike, the dike between the polders and the rest of the land is the secondary dike (fig. 3). The height of the secondary dike is infinite in the model. The consequences are that a flood is not possible in the model. Secondly, when the inlet area is large (thus low friction), is the polder water level the same as the estuary water level. The main interest of this research is the volume of water that can be stored in the polders. The secondary dike should satisfy the requirements of the Delta standard (Roode, 2008), the dike height is thus sufficient to prevent a flood from occurring. Another assumption of the model is a constant polder elevation at mean low water, meaning that no sedimentation will take place in the polder. The consequence is that the model results shows only the initial attenuation capacity and future polder elevation changes are not included.

The model is tested by simulating a tidal wave in the polders. Only later was the storm surge added to model, together with the tidal wave they determine the water level in the Western Scheldt. The aim is to understand the what the effect is on the water levels in the polder and in the estuary.

The model is calibrated and validated with measured water levels from two polders. The calibration and validation are performed over different time periods from the same data series. Estuary water level measurements are used as driver for the model, the data was linear interpolated from 10- to 1-minute frequency data. This is method is correct as one may assume that the water level (1) does not show large variation in 10 minutes and (2) the change in water level within 10-minutes is linear. Rammegors polder has of an inlet consisting of three culverts each with an area of 7m^2. This is modelled as one inlet of 21m^2, combining the three culverts to one. The friction in the inlet underestimated due to this assumption.

As three separate culverts have a higher friction due to the larger surface area. For Perkpolder, an assumption was made regarding the dike width (for the discharge calculation), based on satellite images from the old dike was 10 metres selected. (Google Earth, 2019). Based on the designs of both polders one would expect a higher friction for the culverts at Rammegors polder than for Perkpolder, due to the difference in surface area. With the results from the validation the model can be related to reality and can be assess whether the model functions correctly, which will be done by statistical tests.

When the model was validated, more polders were added to the model to detect a potential threshold level in the storm surge attenuation capacity of the system. The maximal number of polders present in the system is 57, these polders are selected in a previous research (Dubbeldam, 2019). This selection includes only polders with no high valuable assets, reducing costs related to land acquisition.

A ratio is introduced to assess the attenuation capacity of the system. The effectiveness ratio, depending on the polder area and maximal water level in the estuary. Using the effectiveness ratio has its limitations. To apply and use the effectiveness ratio as comparison one should keep the estuary volume constant. Meaning that this ratio cannot be used to compare different sections of the estuary, yet it is correct to analyse the ratios from different polders sizes within one section. The ratio depends on the inlet area and polder sizes of polders present in the estuary. For each different polder area or inlet area should the ratio be recalculated.

To determine when the maximal attenuation capacity is reached, several options are explored. Different variables of polders, size and number of dike inlets have been changed to understand the effect on the attenuation capacity.

Methods

Study Area Western Scheldt

The project Zeeland 2121 is targeted to the whole province of Zeeland, to find a long-term resilient solution to protect the land against the water in the Scheldt. The river Scheldt starts in France and ends 355 km later in the North Sea (Baeyens, Van Eck, Lambert, Wollast, & Goeyens, 1998). From Vlissingen until Antwerp the estuary covers 370 km^2. This research is focused on the Dutch part of Western Scheldt. The width of the estuary decreases from 6 at the inlet to 2 kilometres near Bath, due to this funnelled shaped increases the tidal range from 3.8 at the inlet until 5.2m near Antwerp (Sistermans & Nieuwenhuis, 2004). The mean river is discharge is 100 m^3s^{-1} (Baeyens et al., 1998) which is neglectable with a subtidal volume of $2 \cdot 10^9$ m^3 at the mouth of the estuary (Bolle, Bing Wang, Amos, & De Ronde, 2010; Jeroen Stark, Smolders, & Vandenbruwaene, 2019). The Western Scheldt is can therefore be classified as a meso-tidal dominated system (Baeyens et al., 1998; Sistermans & Nieuwenhuis, 2004).

Figure 1 Satellite image of the Western Scheldt estuary (Google Earth, 2019), located in the south west part of the Netherlands.

Volume based back of the envelope calculation

A simple calculation is done before starting with the model to understand the potential of the double dike system in the Western Scheldt. In the Western Scheldt are 57 polders of different sizes available for a double dike system (Dubbeldam, 2019). Based on this data, the area of the available polders in the Western Scheldt is calculated. The secondary dike height (z_s) is set to +6mNAP, this is the mean elevation of the secondary dike height of the polders (AHN, 2019), from this is the elevation of the polder (p_{elev}) is subtracted. Lastly, the corrected polder height is multiplied with the polder area (A_p) (eq. 1). The volume of the polders is compared with the subtidal volume from a previous study and with the modelled storm surge volume. Assuming that the volume ratio is related to the reduction in maximal water level it is possible to make a first prediction.

[1] $$V_p = A_p * (z_s - p_{elev})$$

Model water flow calculations

The model is created in Python (Python, 2019). Starting with the driver of the model: the tidal and storm surge wave. The water level in the estuary (h) for the tidal and the storm surge wave are both modelled with a sine function (eq. 2). The amplitude (A) of the tidal wave is based on the forecast for Westkapelle at the 27th of September (Rijkswaterstaat, 2019). Using the mean tidal amplitude, halfway between spring and neap tide. The period (P) is 12.416 hours for a semi-diurnal tide. The limitation of using a sine function is the inability to simulate tidal asymmetry and the slight vertical flood dominance in the Western Scheldt (Wang, Jeuken, Gerritsen, De Vriend, & Kornman, 2002). All variables can also be found in Appendix 1, a sketch of the double dike system can be found in figure 3 and appendix 2. The inlet to the polder is situated at mean low water and all the water levels are relative to mean low water [mMLW].

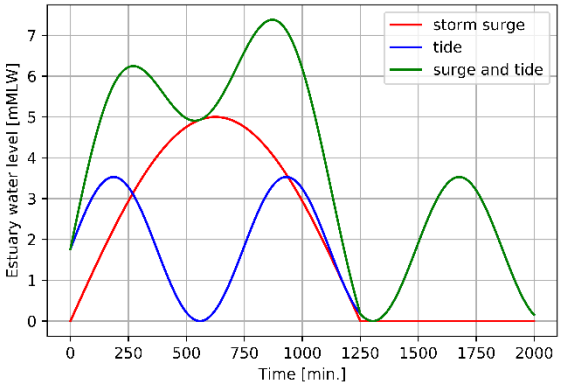

Figure 2 Water level in the estuary relative to mean low water modelled for Vlissingen. The blue line is the modelled tide, the red line is the modelled surge wave. Both estuary water levels are summed for each time step, resulting in the green line. The maximal water level in the estuary (Vlissingen) is reached at t=871 with 5.61mNAP.

[2] $$h(t) = \left(A * \sin\left(\frac{2\pi}{P}t\right) + b\right)$$

The storm surge wave has an amplitude of +5.90mNAP, which is the computational level for a once in $1{\cdot}10^4$ year event (Roode, 2008). The maximal water level of the surge is a few minutes earlier than the tidal wave, hence a slightly lower maximal estuary water level of 5.61mNAP. For the storm surge is the period is set to 24 hours. The sine function becomes negative after a half period, an if-statement is present preventing the storm surge sine function become negative. The next step was to combine the wave height of the tide and the storm surge. The water level was summed for each time step (eq. 3), resulting in figure 2. For the first test is the storm surge equation disabled, only later is the storm surge activated. The storm surge function is disabled when the amplitude is set to zero. The outflow and inflow of the polder are limited by the area of inlet, the Chezy equations are suitable to model the discharge into the polder. These equations have been proven to be suitable for calculations of the inflow discharge into a basin (Kleinhans, 2005). The discharge is determined by the width (w_i) of the dike inlet, sea water level (h) and the flow velocity (u, eq. 4). The flow velocity (eq. 5) depends on the Chezy roughness coefficient (C), depth of the channel (z) (i.e. height of the primary dike) and the slope (S). The Chezy roughness coefficient (eq. 6) is determined by the gravity constant (g) and the friction (f). To calculate the friction the Nikuradse roughness length (k_s) is used (eq. 7: White-Colebrook function), for concrete the roughness length is between 0.001-0.01 m (Dong, Wang, Zhao, Liu, & Liu, 2001; Streeter & Wylie, 1985); using 0.05m. The slope is the driver in the Chezy equations of the discharge. The slope is calculated (eq. 8) as the difference between the sea level (h) - measured from mean low water - and the polder water level (h_p) divided by the width of the primary dike (x_d). The estuary water level (h) is driven by the combination of the storm surge and the tidal wave, the polder water level (eq. 9) is calculated by the discharge (Q) into the polder and the polder area (A_p).

[3] $$h(t) = \left(A * \sin\left(\frac{2\pi}{P}t\right) + b\right)_{tide} + \left(A * \sin\left(\frac{2\pi}{P}t\right) + b\right)_{storm\ surge}$$

[4] $$Q = u * h * w_i$$

[5] $$u = C\sqrt{z * S}$$

[6] $$C = \sqrt{\frac{8g}{f}}$$

[7] $$\sqrt{\frac{8}{f}} = 5.75 \log_{10}\left(\frac{h}{k_s}\right) + 6.24, \quad f = \frac{1}{8}\left(\log_{10}\left(\frac{h}{k_s}\right) + 6.24\right)^2$$

[8] $$S = \frac{h - h_p}{x_d}$$

[9] $$h_p = \frac{\sum Q}{A_p}$$

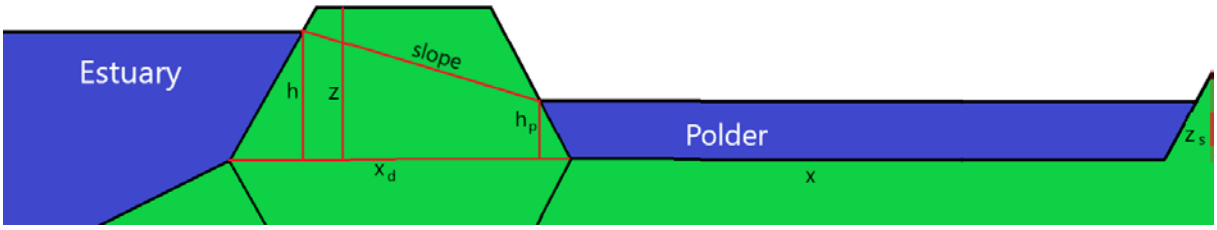

Figure 3 Sketch double dike system, side view. On the left-hand side, the estuary water level (h), on the right-hand side the polder water level (h_p). The primary dike is located between the polder and estuary with a height z and width x_d. The slope is the difference between the water level of the estuary and polder divided by the width of the polder. On the right hand-side, the secondary dike is present, with a height z_s. The polder elevation is located at mean low water. The water flow between the estuary and polder is calculated with the equations of Chezy.

If the water level in the polder becomes higher than in the sea level, the slope will become negative. This results in negative discharge (i.e. outflow) and a decreasing water level in the polder. The dike height (z in eq. 3) is dependent on the inlet area, the inlet area is set to 60m^2 as default, later during my research different inlet areas were tested.

To capture the different sizes of the polders present in the Western Scheldt are the polders sizes in the model based on data from polders in the Western Scheldt (Dubbeldam, 2019). To correctly model the polder sizes, it would be preferable to use the mean (μ) and the 95% confidence intervals (+/-2σ) from a normal distribution. The central limit theorem states that a population with a sufficient number of random samples from a population can be approximated by a normal distribution (LaMorte, 2016; Ott & Longnecker, 2015). However, the Western Scheldt holds only 57 available polders. The statistics are applied to the data from both the Scheldts (n=142), increasing the sample size and thus increase the statistical reliability (Calkins, 2005). Finally, a test of normality was performed in SPSS (Appendix 3) (SPSS, 2017). Only the logarithmic transformed areas from the Western Scheldt passed the significance level of 0.05, meaning that this is a normal distribution (Appendix 3). With an upper 95% confidence bound at 6.0455, lower at 5.7507 and the mean at 5.8981, resulting in the areas in table 2. The polder area is rounded off to the nearest ten thousand.

Table 1 Recalculated polder size dimensions from the Western Scheldt data. A classification is made between the polder sizes based on the statistics of the logarithmic transformed areas in SPSS. The medium polders are the mean, the small and large polders are the lower and upper 95% confidence interval.

Number	Normal distribution	Name	Polder Area [m^2]	Polder width [m]	Polder length [m]
1	Lower 95% (μ-2σ)	Small	560,000	560	1000
2	Mean (μ)	Medium	800,000	800	1000
3	Upper 95% (μ +2σ)	Large	1,100,000	1000	1100

Understanding if and how the location of the polder effects the attenuation capacity, there should be the possibility to add a spatial scale to the model. Creating insight in potential non-linearity in the attenuation capacity along the Western Scheldt. Hence the model is divided in parts, splitting the Western Scheldt in an inlet, mid and upstream part (fig. 4). The inlet part is defined by an infinite water volume, representing the sea, which is greatly exceeding the polder volume. Therefore, is assumed that the water volume entering the polders has an insignificant influence on the water level of the sea, thus addition of polders will not reduce the water level. No further calculations are performed on the inlet section of the Wester Scheldt. For the mid and upstream part, water volumes are calculated, as shown further on. The amplitude of the tidal wave is increased upstream due to the funnelling effect of the relatively shallow Western Scheldt estuary (Wang et al., 2002). The factor at which the tidal amplitude is increased, is calculated with the use of water level measurements at Vlissingen, Hansweert and Bath. The amplification is calculated by dividing the estuary water at Hansweert (mid-section) by the Vlissingen estuary water level. Upstream the water level measurement from bath used (Rijkswaterstaat, 2019). The amplification factors are calculated for a spring (14-12-2019 09:25 UTC+2) and neap tide (21-12-2019 15:18 UTC+2), resulting in 1.1 midstream and 1.4 upstream.

Figure 4 Sections of the Western Scheldt estuary (Google Earth, 2019). The Inlet section is characterised by a large estuary volume, modelled as infinite (e.g. the sea). For the mid- and upstream sections is the water volume calculated based on the area of the estuary.

Sensitivity test for k_s

The parameter for the roughness length of concrete is an assumption, hence the need to check whether it is an acceptable assumption. The Nikuradse roughness length used in the friction calculation is the mean from a range of values found in literature. To test whether it is correct to assumption is the mean value compared with the extreme roughness lengths for concrete (0.01 and 0.001 m). An analysis showed how much this effects the calculation of the Western Scheldt water level. The water levels of the Western Scheldt are calculated for the situation of ten large polders, with varying roughness lengths. A SPSS test (appendix 6) showed that the water levels from extreme k_s values (0.01 and 0.001 m) fall within the standard error of water levels calculated by the mean roughness length value. Therefore, concluding that the mean value of 0.005m is an appropriate solution.

Water Balance Calculation

In this conceptual model are the sections and polders represented as boxes with a certain volume of water. The volume of water is used to calculate the water level in the polders or in the Western Scheldt. In this section will be explained how the volume of water in the polder and estuary are calculated in the model. Later in the research is the tidal wave is selected as driver for the model, for the period 01-11-19 – 01-12-19 (Rijkswaterstaat, 2019). After, water levels in the estuary were calculated by the model. Different simulations were performed with varying inlet areas. The goal was to understand how the dimensions of the inlet will impact the tidal range and water flow in the polder.

Estuary water volume calculation

The volume of the estuary is calculated via a water balance, the volume in the Western Scheldt is the volume entering minus the volume leaving. Volume is calculated (eq. 10) based on the estuary water height (h), the width of the estuary (w_e) and the length of the section (L) (Van Rijn, 2010). The volume is calculated for both the mid and the upstream Western Scheldt section. In the model is the area of the Western Scheldt calculated from the high-water line, however, 20% of the estuary is inter tidal area (de Jong & de Jonge, 1995). The water volume is calculated relative to mean low water, but using the high-water line resulting in an overestimation of 20%. The calculated volume will therefore be compared with values found in literature.

The water volume leaving the estuary leaving depends on the discharge (Q) into the polders (eq. 11). The discharge is calculated with equation 3. If there is more than one polder, the discharge is multiplied with the number of polders (p_x). The subscript s, m or l indicates the size of the polder, respectively small, medium and large. The sign of the discharge is determined by the slope, a negative discharge indicates water moving from the polder into the estuary.

[10] $$V_e = Q_{in} - Q_{out} = (w_e * L * h) - \sum Q$$

[11] $$\sum Q = Q_s * p_s + Q_m * p_m + Q_l * p_l$$

The water volume of the subtidal wave is calculated (eq. 10). The water volume depends highly on the location as the width of the estuary decreases exponentially upstream. The area from Vlissingen to Breskens (4 km) is chosen, because literature was available on the subtidal water volume from this location, which is used as a comparison (Baeyens et al., 1998; Bolle et al., 2010; Jeroen Stark et al., 2019). Using equation 10, the water volume of the estuary was calculated. The modelled storm surge volume is larger than the subtidal volume modelled by Stark et al., (2019). The difference is too large, even though the storm surge wave is expected to be a bit higher than the tidal wave. The calculated storm surge water volume is an overestimation, roughly 11 times. The modelled tidal water volume is an overestimation. The tidal water volume is recalculated by multiplying the volume with a factor (eq. 12) The area of the sections is scaled with a factor (f_x) to correct the total subtidal volume: f_m 0.087 is and f_{up} is 0.09.

[12] $$f_x = \frac{V_{calculated}}{V_{literature}}$$

Table 2 Water volumes calculated in the model and compared with literature data

Location Western Scheldt	Source	Volume	Water Volume [km^3]
Polder	Model	Polders	∞
Mid	Model	Subtidal	23
Up	Model	Subtidal	6
Mid	Literature[1]	Subtidal	2.01
Up	Literature[1]	Subtidal	0.541
Mid- and upstream	Model	Storm Surge	4.903

[1](Baeyens et al., 1998; Bolle et al., 2010; Jeroen Stark et al., 2019)

Water level calculation

The water level in polders is calculated by dividing the total volume of a specific polder size by the total area of these polders (A_p) (eq. 13). The calculation is done each time step [min], the discharge (Q_x) [m^3/min] is than in the same unit as the volume [m^3]. The water levels are calculated for each polder size separately. For the estuary (eq. 14), is the water volume (V_e) divided by the area of the Western Scheldt; length (L) times the width (w_e) of the section. Both water levels are relative to mean low water, assuming that the polder elevation is at mean low water.

[13] $$h_p = \frac{Q}{A_p}$$

[14] $$h = \frac{V_e}{L * W_e}$$

Calibrating the friction in the model

The friction value used in the discharge calculation was an estimation, to correctly estimated the friction was the model calibrated. Using measurements from a similar sized polder as in the double dike system, data from the Rammegors polder and Perkpolder. The polders are recreated in the model and the friction is used as the calibration parameter. The driver for the model is the tidal wave, measured data from the estuary water level (Rijkswaterstaat, 2019), measured in a 10-minute frequency. Using linear interpolation, the dataset was converted to a 1-minute frequency. The data in the polder is measured by divers (Reefnet Sensus Ultra) which measured the pressure each minute. All the data was given in pressure (mbar), for the conversion into polder water depth (h_p) in metres was equation 15 used. p is the measured pressure, p_0 is the air pressure both in mbar. The air pressure data was taken from a weather station near Vlissingen, a dataset containing daily measurements (KNMI, 2019). The difference in pressure is divided by the density of water (ρ = 997 km/m^3) times the gravity constant (g = 9.81 m/s^2). The water level is added by the height of the diver above NAP (z_0).

[15] $$h_p = \frac{p-p_0}{\rho * g} + z_0$$

The model calculated the polder water levels for a range of friction values. The modelled and the measured water levels were compared. The final friction value is the value that best predicted the measured water level. In order to make conclusion on the validity of the model calculations was the r-square, root means square error (RMSE), the bias and the Index of Agreement (IoA) used (Callaghan et al., 2010). In the IoA (eq. 16) is x is the modelled data, y is the observed data and an overbar ($\bar{x}, \bar{y}$) indicate the mean value. If the index value is closer to one, is the water level amplitude better predicted by the model. Values outside the range of 0 – 1 indicate situations when maximal or minimal water levels are badly predicted. Using the root means square error (RMSE) determine the absolute difference between the model (x) and observed data (y) (eq. 17). The optimal outcomes would be a low RMSE. Calculating the RSME and r-squared is the sklearn.metrics package was used (Python, 2019). The correlation coefficient is calculated with equation 18 (Taylor, 2001), later the outcome is square to compute R^2. An R^2 of 1 means a perfect correlation. The bias (eq. 19) is calculated as the difference between the mean of the modelled ($\bar{x}$) and the observed data ($\bar{y}$) (Kärnä & Baptista, 2016; Taylor, 2001). A smaller bias is indicating less variation and thus a better prediction. Based on the listed statistical tests, the best approximation of the friction value was selected. Calibration plots can be found in Appendix 7.

[16] $$IoA = 1 - \sum(x-y)^2[\sum(|\, x-\bar{y}\,| + |\, y-\bar{y}\,|)^2]^{-1}$$

[17] $$RMSE = \sqrt{\frac{\sum(x-y)^2}{n}}$$

[18] $$R = \frac{1}{\sigma_x \sigma_y}\frac{1}{N}\sum_{n=1}^{N}(x_n-\bar{x})\,(y_n-\bar{y})$$

[19] $$BIAS = \bar{x} - \bar{y}$$

Rammegors

Rammegors polder is located in the Eastern Scheldt (appendix 8), created to prevent sediment starvation by allowing the water to enter into the polder (Jentink, 2015). The dataset used for the calibration and validation is the same, however for the validation is a different timeseries used. The calibration data series range from 05-12-14 till 10-12-14 (12:40:00 - 09:20:00 UTC+2). Measurements of the polder water level were performed at three locations, location 2 is used as it best reflects the water level in the deep part of the polder. The Rammegors polder is limited from 0.50 to 1.65mNAP due to the polder elevation and closing culverts at high water. This is modelled with an if-statement in the script, preventing the water level going below the mean polder elevation. The estuary water level measurements are taken from Sint Annaland Haven Steiger (Rijkswaterstaat, 2019), located 5 kilometres to the west. Table 4 lists the values of the parameters for the specific polders in the model. The inlet area, polder area and dike width are measured based on satellite images (Google Earth, 2019).

Table 3 Input parameter values for the polder simulation in the model.

Rammegors		Perkpolder	
Parameter	*Value*	*Parameter*	*Value*
Inlet Area (A_i)	21 m^2	**Inlet Area (A_i)**	400 m^2
Polder Area (p_a)	396,000 m^2	**Polder Area (p_a)**	648,000m^2
Dike width (x_d)	60 m	**Dike width (x_d)**	60 m
Mean polder elevation (b)	0.50 m	**Mean polder elevation (b)**	0.60 m

The uncalibrated model was not able to predict the water level well. The water levels move far away from the 1:1 line, large over- and underestimation. During the calibration is the friction selected based on the highest r-squared and IoA in combination with a small RMSE and bias. Eventually, 1.43 is used for the friction value (table 4).

Perkpolder

The perkpolder data is used as a second calibration for the model. This area is just recently transformed into polder with the aim to stimulate recreation, social and economic activity (Ginkel & Mooyaart, 2012). Besides the positive effect on the local economy is this polder a perfect test case for the model.
This low-lying polder has inlet width of 400 meters. The polder is simulated in the model using the data from table 4. Again, using the measured estuary water level as the driver for the model. The water level of the estuary is taken from Walsoorden measurement location (Rijkswaterstaat, 2019), roughly 300 meters north of the inlet. The Perkpolder data ranged from 21-06-16 until 28-06-16 (10:04:00 - 17:04:00 UTC+2), the water levels at Walsoorden from the same period are used as input for the model. The pressure is measured at four locations (appendix 9), for each diver is the water level calculated with equation 15. Once concerted to water depth, area all the water level averaged in the Perkpolder. Using the mean water level because all the measurement equipment is at roughly at the same elevation. By averaging the water levels the goal was to reduce potential measurement errors or other disruptions in the signal. The water levels in the polder was calculated for a range of friction values, subsequently, the RMSE (eq. 17), Index of Agreement (eq. 16), bias (eq. 19), and r-square value (eq. 18) were calculated. Based on the statistical parameters, the best approximation of the friction value is 0.35 (table 4).

Table 4 Results statistical test for the calibration of the Rammegors and Perkpolder, respectivally f = 1.43 and f = 0.35.

Calibration	RMSE [m]	R^2	Index of Agreement	BIAS [m]	n
Rammegors	0.234	0.791	0.939	0.157	7,000
Perkpolder	0.137	0.964	0.992	-0.007	10,500

The difference in friction value can be attribute towards the design of inlets. Perkpolder has a large inlet in the dike while Rammegors has three small culverts. The higher friction in Rammegors is explained by the smaller inlet and the vegetation in the polder, which reduce the flow velocity.

Validating the calibrated model

Following on the model calibration in the previous section, the model is checked whether the calibration is correctly performed. In this section is the friction calibration validated, with another time period in the same dataset. The model should be able to function outside the calibration period. In this validation process, estuary water levels are used as input for the model. The water levels calculated by the model will be checked with measured data from the polders. Using the RMSE, r-square, bias and IoA to quantify the measure of prediction. The Rammegors validation is performed over the period of 12-12-14 to 16-12-14 (03:00:00 - 23:40:00 UTC+2), the Perkpolder from 04-07-16 to 28-08-16 (06:24:00 - 19:44:00 UTC+2). The validated timeseries of the measured and modelled water levels can be found in appendix 10.

Rammegors

The Rammegors validation is shown in figure 5, the water level follows reasonably the 1:1 line. The maximal water level is an underestimation compared to the measured water level. Maximal water levels in the polder are being underestimated from a few centimetres till almost 30 centimetres. There seems to be a bias towards an overestimation at measured water levels below 1.0m, an underestimation for high water levels. The over and under estimation is reflected in the relatively high the bias (table 5).
The timing of the modelled ebb and flood agree with the measurements (appendix 10). However, the polder drains slower than the model predicts, the time to fill the polder is similar in the model and measurements. The statistics (table 5) substantiate a good correlation. The model slightly underestimates the maximal water levels in the polders. But, the overall correlation between the modelled and measured water level is good.

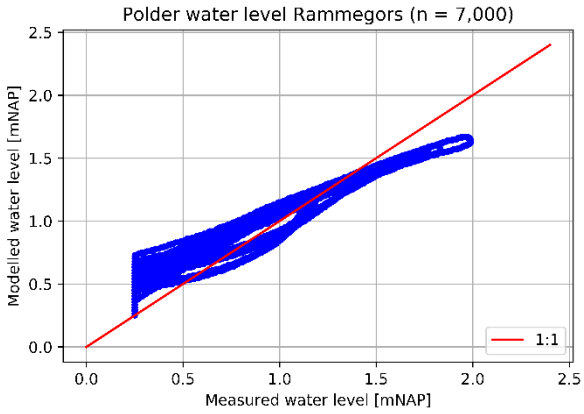

Figure 5 The blue dots are the measured water levels in the Rammegors polder and modelled water levels by the model. The red line (1:1) indicates a perfect fit. The model overestimates the water levels below 0.5m and underestimated water levels above 1.5m. The validation is preformed over 7,000 minutes.

Perkpolder

The model follows the 1:1 line, a good prediction for the Perkpolder water level. Table 5 for the results of the statistical tests. The Index of Agreement is high (0.993), indicating that the amplitude (i.e. minimal and maximal water levels) is correctly predicted by the model. For measured water levels lower than 2 metres water levels is the model showing more variation, compared to higher water levels. This variation is an underestimation by the model, confirmed by the negative bias (table 5). The high r-squared value can indicate a larger bias in the data set, however from figure 6 and table 5 this does not seem to be the case.

The sample size of the two cailbrations differs, the sample size of the Rammegors polder was smaller than Perkpolder, but both sample sizes are sufficient to provide a useful statistical outcome (Bujang & Baharum, 2016). Based on the two validations executed, is the Perkpolder calibration parameter value (f = 0.35) used. Meaning the highest r-square, lowest RMSE, highest IoA and the lowest bias. Also, the Perkpolder validation could be executed over a longer time series, increasing the statistical reliability (Calkins, 2005). To ensure a better approximation of the friction value one could use more data sets for the calibration process.

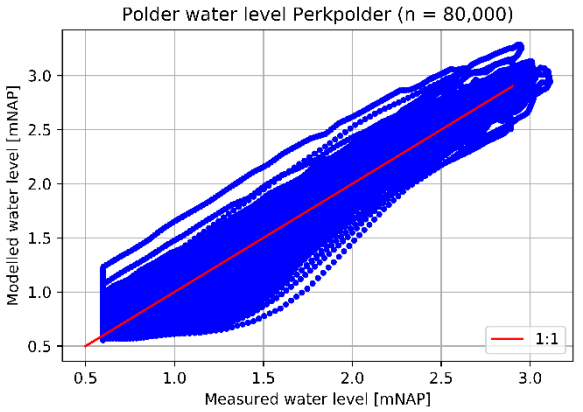

Figure 6 The blue dots are the measured water levels in the Perkpolder polder and modelled water levels by the model. The red line (1:1) indicates a perfect fit. The validation is preformed over 80,000 minutes. The model follows the 1:1 line, however there is more variation.

Table 5 Results statistical tests for the validation

	RMSE [m]	R^2	Index of Agreement	BIAS [m]	n
Rammegors	0.206	0.825	0.959	-0.136	7,000
Perkpolder	0.122	0.972	0.993	-0.0231	80,000

Effectiveness ratio

In this research is the Western Scheldt is used as a test case. A double dike system has the potential to be applied in delta's worldwide. If the attenuation potential of this system could be estimated easily, the threshold to investigate and implement such a system would be lowered. The developed model requires as input only a few simple parameters, most of them can be found in literature. To understand the outcomes of the model, a ratio is introduced. When the ratio is set out against the maximal estuary water level it is possible visualize the relationship. Detect any non-linearities between the attenuation capacity and the polder or inlet dimensions.

To understand the relationship between the area of the polder and the water level in the Western Scheldt, a unitless ratio is created, called *effectiveness*. The ratio is based on the maximal water level in the estuary (h_{max}), the total polder area (A_p) and the volume of the estuary (V_e) in order to visualize the relationship (eq. 20). In an ideal solution is the polder area and the maximal water level small compared to the volume of the estuary, hence preferable a larger ratio. This ratio is calculated for all polder sizes while varying the number of polders from 1 to 57.

[20] $$effectiveness = \frac{V_e}{h_{max} * A_p}$$

Results

Volume based back of the envelope calculation

First, using a simple equation to calculate the volume of all the polders in the Western Scheldt results in 0.407km^3. The total subtidal volume of Western Scheldt near Vlissingen is 2.01km^3 (Bolle et al., 2010; Jeroen Stark et al., 2019). This raises the question: what is the effect of adding polders which are only 25% of the volume subtidal volume? Assume that the reduction in maximal wave height is directly related to the volume of the estuary and the polders, thus an 25% reduction in maximal water level. For example, a storm surge wave of 5mNAP would be reduced to 4.00mNAP and a surge wave of 7mNAP could be reduce to 5.60mNAP. Based on these two examples it seems that the water storage increases from 1.00m to 1.40m. Again, this is a simplified first calculation. In the next sections are the model results presented.

Tidal wave test

In the first simulations was the storm surge function disabled, with the aim to analyse how the model functions during normal conditions. Polder water levels were calculated by the model based on input. Input for the model was a tidal wave, measured at Vlissingen and Bath by Rijkswaterstaat (2019). Representing the mid and upstream estuary sections. Figure 7 shows the tidal wave in the polder and estuary; the solid yellow line is the measured water level in the Western Scheldt near Bath. The dotted lines are the water levels in the polder calculated by the model, for an inlet area of 30m^2 upstream in the estuary. The tidal range is reduced in the polders, the highest tidal range can be found in the smallest polder. If the tidal range in the Western Scheldt is lower, during neap tide (06-11-19), the difference in water levels between the estuary and polder are reduced. Next, there is lag in the time when the maximal water level is reached, the maximal water level in the small polders is reached when the water level of the estuary has already started to drop. The size of the inlet area determines the lag and the tidal range in the polders. Further, the tidal amplitude depends on the polder size. The discharge into the polders is equal but for a smaller area needs the polder water level to be higher to store the same amount of water volume.

The lag and reduced tidal amplitude in the polder can be attributed towards the dimensions of the inlet, increasing the inlet area reduces the lag and increase the tidal amplitude in the polder. For a large (>100m^2) inlet area there is no lag between the maximal water level in the estuary and polder. Also, the tidal amplitude in the polders is equal to the estuary amplitude. The same results apply to the midstream Western Scheldt (appendix 11).

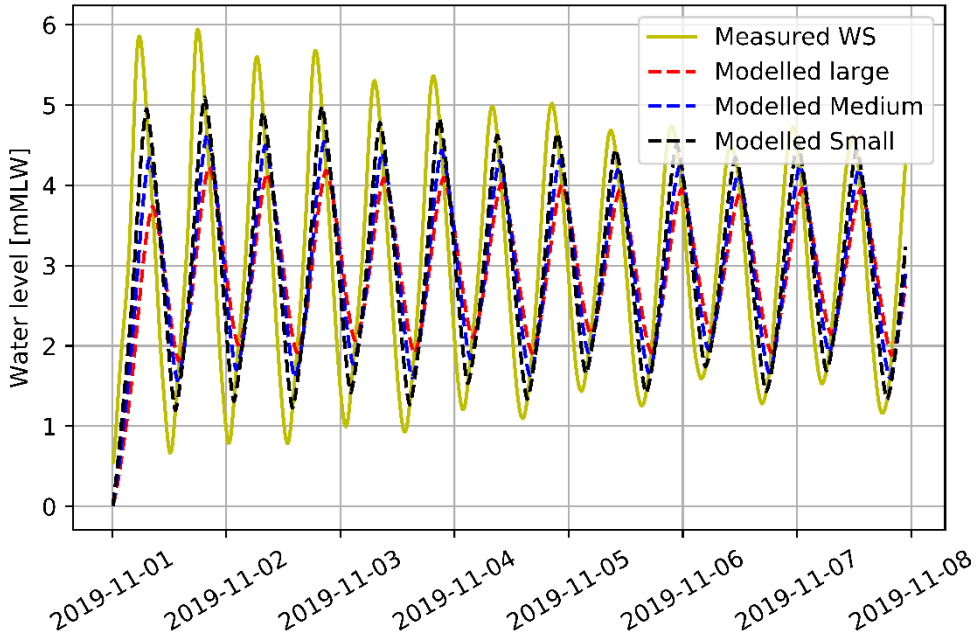

Figure 7 Modelled water levels in the polders and Western Scheldt for a normal tidal wave. As input are the estuary water level measurements used from Bath (Rijkswaterstaat, 2019).The solid yellow line indicates the measured water level in the Western Scheldt, relative to mean low water. The coloured dotted lines indicate the modelled polder water level in a specific polder size upstream in the estuary. The polder water levels are calculated for three separate simulations; 3 large, 3 medium and 3 small polders with an inlet area of 30m^2. The tidal amplitude in the polders is reduced compared to the estuary. Further, the tidal amplitude in the polders depends on the size of the polder.

The attenuation capacity

The model can predict the water levels in the polder during normal conditions, next is the storm surge is activated. In this section is the goal is to find the combination of parameters which lead to the biggest reduction in maximal water level. At first understand the effect of the number of polders, later is the effect of the inlet area analysed. Analysis is supported by a ratio, creating insight with a relatively simple solution. The last part presents an optimal solution based on the produced results.

Polder area

The total polder area is kept constant to understand the effect of polder area. Starting with a simulation of an equal total polder area, three large polders are used as reference. Simulations with different sizes of polders are performed (table 6). Comparing the water levels in the Western Scheldt with the default run, it becomes obvious that the reduction in surge wave height is in the order of centimetres for this specific simulation. Secondly, the smallest sized polders provide the most attenuation capacity. Here should be noted that the small polder area is not precisely the half of a large polder area, to get an integer the value (5.89) is rounded up to 6. Hence, the change in water level for the small polder is bit overestimated, therefore this data is only used as a first suggestion.

Table 6 Simulations with a total equal polder area with an inlet of 60m^2, water level measured from mean low water

Polder classification	Number of polders	Water level [m] Western Scheldt Mid	Change in water level [%]	Water level [m] Western Scheldt Up	Change in water level [%]
Default		*6.886*		*10.116*	
Large	3	6.883	0.04	10.101	0.15
Medium	4	6.883	0.04	10.096	0.20
Small	6	6.881	0.07	10.084	0.32

Adding more polders results reduces the maximal water level in the Western Scheldt (fig. 8). The y-axis is the maximal estuary water level, relative to mean low water. The solid lines represent the mid estuary and the dotted lines are the upstream estuary. The colours refer to the size of the polder present in the system.
The overall trend at the midstream location: larger polder areas results in a lower maximal water level, because more volume is available for water storage. However, the difference in attenuation capacity between the polders is limited. Also, the overall attenuation capacity is small compared to the upstream estuary. The same number of polders upstream results in a larger attenuation capacity, also is the difference between the polder sizes more pronounced. Simulations with larger inlet areas results in the same pattern (appendix 12).
The attenuation is related to the total polder area. Small polders have roughly 0.75 the polder area of the large polder. Yet, comparing the reduction in maximal water level for 10 large polders with 13 small polders, we see that the reduction is equal for both polders. So, for a similar total polder area there is an equal attenuation capacity. Next, is the effectiveness ratio applied to further investigate this finding.

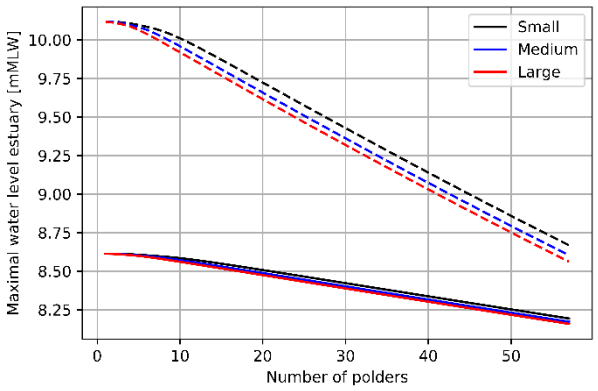

Figure 8 Maximal water levels for the mid (solid) and upstream (dotted) estuary. The maximal water levels in the estuary are modelled for a range of polder numbers (x-axis) and different sizes of polders. Increasing the number of polders decreases the maximal water level in the estuary. The decrease in maximal water level is more pronounced in the upstream section of the estuary.

Effectiveness

Applying the effectiveness ratio to this data shows that the large polders (60m^2) have the highest ratio (appendix 13). Both in the mid- and upstream is an exponential increase in the ratio with the number of polders. When increasing the inlet to larger value (>200m^2), there is a linear increase in the ratio for an increasing number of polders. Increasing the inlet area further, leads to an exponential increase in the effectiveness ratio. This occurs because more volume can be stored in the polders, reducing the maximal water level in the estuary and increasing the denominator is the ratio. When the optimal inlet area is reached, the effectiveness ratio has a maximum. In all simulations have the large polder the highest ratio, the difference between the other polder sizes in ratio is small. The largest number and size of polders results in the highest attenuation capacity.

Inlet area

Analysing the effect of the inlet area on the attenuation capacity was performed by varying the inlet area, while keeping the number of polders constant at 57. Figure 9 shows the results, the dotted line for upstream and the solid line for mid-Western Scheldt. The y-axis is the maximal water level in the estuary (e.g. the solid black lines indicate the maximal water level in the Western Scheldt for 57 small polders with a certain inlet area, x-axis). The general trend in the data is a decreased maximal water level for an increase in inlet area. More specific, the decrease in maximal water in level (mid-section) is slightly exponential, for large inlet areas is the reduction in maximal water level the highest. Polder in the upstream estuary reach around 220m^2 their maximal reduction in estuary water level. The reduction in estuary water level is larger in the upstream part of the estuary. The difference between the sections exists due to a difference in estuary volume, upstream is the estuary volume relatively small, thus less polder volume needed to reduce the water level.

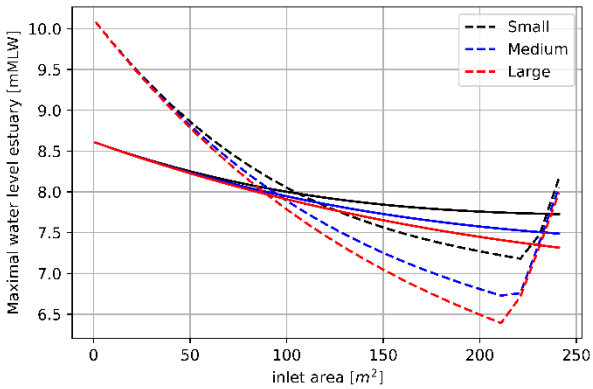

Figure 9 Maximal estuary water levels modelled for 57 polders with varying inlet areas (x-axis). The solid line is the mid estuary and dotted are maximal estuary water levels for the upstream part of the estuary. Increasing the inlet area reduces the maximal water level in the estuary, until a certain size (e.g. 215m^2 for large polders upstream). The reduction in the maximal estuary water level is the largest for the upstream estuary with the large polders.

The inlet areas with maximum attenuation capacity are listed in table 7. Even though, the inlet area of the polders midstream is at least twice as big, the attenuation capacity is not. The attenuation capacity of the double dike system upstream is for each situation higher than it is midstream. This means that the inlet area and location determine the attenuation capacity.

Table 7 Optimal polder inlet areas for different polder sizes and locations, at this inlet area is the maximal attenuation capacity reached.

Polder size	Optimal inlet area [m^2]	
	Midstream	*Upstream*
Small	450	230
Medium	550	215
Large	680	210

A limitation of this simple model is shown in figure 9, there seems to be an optimal inlet area. The attenuation capacity increases until this value and decreases beyond this value. Increasing the inlet area decreases the friction on the water flow. A larger inlet area should allow more water to flow in and out of the polder. At a specific moment is the inlet area no longer determining the attenuation capacity, a different factor has become limiting. As result is a maximum attenuation capacity reached after a certain inlet area size. Increasing the inlet area further should not influence the attenuation capacity, the capacity should stay the same. The reduction in attenuation capacity for large inlet area is counterinitiative. A possibility might be the time step in the model, if the 1-minute step would be too course. However, simulations with a 1-second time step results in the same pattern. This error may be attributed the model equations and not the time step chosen in the model simulations.

Highest attenuation capacity for the Western Scheldt

Previous results have shown the of potential attenuation capacity. However, which combination of factors leads to towards a maximal reduction in estuary water level? The results so far indicated a far stronger attenuation potential for the upstream Western Scheldt as the estuary volume is smaller, accordingly are the upstream Western Scheldt options further explored. Along the Western Scheldt are 57 polders available, assuming that half is located in the upstream section, there are 28 polders available. To find the inlet area at which the reduction in the estuary water level is the largest, is the inlet area varied. The optimal inlet areas differ from table 7 as the total number of polders has been changed in this simulation.

The highest reduction in estuary water level is reached for 28 large polders (fig. 12) with an inlet area of 297 m^2. However, to determine the attenuation capacity for the Western Scheldt one should look at the medium sized polders, these are based on the mean polder area of polders in the Western Scheldt. The inlet area that results in the highest attenuation capacity of 28 medium polders is 197 m^2. This situation leads to a reduction of 11.6%, a maximal estuary water level of 8.94mMLW (7.2mNAP).

During these simulations a numerical issue has come to light, visible in figure 12; black dotted line for an inlet area larger than 270m^2. More information in appendix 15 on the numerical error. The error did not influence the results presented here.

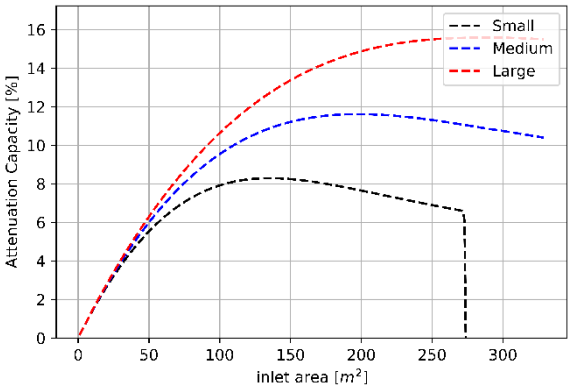

Figure 10 Attenuation capacity of a double dike system for a varying inlet area (x-axis). The attenuation capacity is the percentual decrease in maximal estuary water level compared to a simulation without polders present. The attenuation capacity is calculated for 28 polders of different sized (dotted lines). The attenuation capacity increases exponential until a maximum is reach. The largest attenuation capacity is for 28 large polders with an inlet area of 297m^2upstream in the estuary. The medium sized polders best reflect the situation in the Western Scheldt, maximal attenuation capacity of 11% is reached at an inlet area of 197m^2.

Discussion

Main findings

The goal of this research was to get a first insight on the storm surge wave attenuation capacity by a double dike system in the Western Scheldt. The storm surge and tidal wave can be modelled with a sine function, the interaction between the polder and estuary volume is described by the flow equations of Chezy. The model was able to calculate the discharge at the inlet and the water level in the polder and estuary. In the model was the friction used as calibration parameter and validated with a different dataset, with good results from statistical tests. The model can predict the tidal amplitude in the polder based on water level measurements from the estuary.

The effectiveness ratio was used to show that the polder size is irrelevant for smaller inlet areas (<60m^2), increasing the inlet area further resulted in a difference in attenuation capacity. The ratio may help understanding the relationship between the double dike design and attenuation capacity. However, it is not possible to determine the attenuation capacity based on the ratio alone.
The largest polders have the highest attenuation capacity. The relationship between the number of polders and attenuation capacity starts exponential and quickly transforms into a linear relationship. The number of polders should be as large as the area allows to ensure maximal attenuation capacity.

The inlet area of the polder is mainly determining the attenuation capacity. However, the attenuation capacity reaches a maximum at a certain inlet area. The optimal inlet area of a polder is determined by the polder size and location and the number of polders present in the system. The larger the polder size is, the larger the inlet area is at which the maximal attenuation capacity is reached.

A large-scale double dike system in the Western Scheldt is able to attenuate part of the storm surge wave. This is the first research that has shown the potential for a large-scale application of a double dike system in the Western Scheldt.

The maximal reduction in estuary water level during a storm surge is 11%, based on 28 medium sized polders with an inlet area of 197m^2 upstream in the Western Scheldt. Compared to the back of the envelope calculation (25%) this is lower, difference is due to the addition of friction in the model. The difference is significant and therefore one cannot ignore the friction in the calculation. The model has provided a better result than the first calculation, even though assumptions have been made. The most important assumptions will be discussed.

Assumptions

Chezy equations

The Chezy equations have proven to be effective to predict water flow (Kleinhans, 2005; Zhou, Bao, Li, Cheng, & Bao, 2018). The calculation of the friction with the White-Colebrook function is commonly used (Kleinhans, 2005; Marra, Braat, Baar, & Kleinhans, 2014), but is known to be less accurate when laminar water flow transitions into turbulent flow (Zeghadnia, Robert, & Achour, 2019). Also, is the friction a result of complex interactions (Kleinhans, 2005; Zeghadnia et al., 2019) and therefore difficult to estimate beforehand the correct value. In the past it has been proven that the friction depends on the Reynolds number, relative roughness, etc…(Rouse, 1965) Too complex to apply in the this 1D model. This is less relevant for this research because (1) it is correct to assume turbulent water flow, (2) the goal was to create a simple model and (3) the friction is calibrated and thus did not used the White-Colebrook function in the final calculations.

Secondary dike height

The storm surge height in the model is based on the computational level for a $1/1{\cdot}10^4$ year event, the Delta-standard would be sufficient for now. However, there are serval arguments in favour for an increased dike height. For 2100 is 0.84m of sea level rise expected (Pörtner et al., 2019). Model simulations have showed that the storm surge wave height can increase up 10-20% by 2100 for the North Sea (Beniston et al., 2007; Vousdoukas, Voukouvalas, Annunziato, Giardino, & Feyen, 2016; Woth, Weisse, & von Storch, 2006). An increase in mean sea level could also increase the tidal range, due to the large surface area of the Western Scheldt (Leuven, Pierik, Vegt, Bouma, & Kleinhans, 2019). Continuously dredging in Western Scheldt increases the tidal prism (de Vet, van Prooijen, & Wang, 2019; Van Rijn, 2010). The secondary dike height should be increased when developing a long-term sustainable solution, like the double dike system. The recommendable dike height is the Delta standard plus the expected sea level rise for 2100, 0.98m for the business as usual scenario (RCP8.5 IPCC), thus 7mNAP.

Estuary water volume

The modelled and scaled estuary water volume are compared to values found in previous researches (Baeyens et al., 1998; Bolle et al., 2010; Jeroen Stark et al., 2019). The modelled water volume was 11 times higher than previous studies found. The difference between the modelled and observed volume can be explained by the chosen area to calculate the Western Scheldt volume. Ignoring the shallow intertidal areas and as result largely overestimating the average depth in a cross section led to the volume overestimation. Using data from previous studies was justified based on the discrepancy between the modelled volume and the volumes found in multiple previous researches.
The maximal water level reached in the upstream estuary, is extremely high. A surge wave of 6 meters, 1.4 times amplified due to the funnelled shaped estuary and taking place during flood. This water level is at current day highly unlikely to be reached, however in the future these water level may be reached. This extreme water level was used to show the potential of the system.

Sedimentation

This model ignores sedimentation, however sedimentation in an estuary can have a significant impact. Sedimentation rates are around 1.7 cm/year in the Western Scheldt tidal flats (Zwolsman, Berger, & Van Eck, 1993). In a recently opened polders in the Western Scheldt are rates measured in the first months of 60-400 cm/year (Oosterlee, Cox, Temmerman, & Meire, 2019). This indicates the importance of effect of sedimentation. Increasing sedimentation in the polder, reduces the volume and thereby the attenuation capacity. This could be solved of accepted, both options will contribute to enhanced coastal safety. The solution could be a control reduced tide system (CRT). This system allows the water flowing in only during high water levels (e.g. storm surge) and the outflow from the polder is via a culvert. This culvert is located at the same elevation as the polder, meaning that outflow of water is possible when the estuary water level is lower than the polder elevation (Cox et al., 2006). The control reduced tide system limits the sedimentation in the polder to a minimum (Jacobs et al., 2009; Maris et al., 2007; Oosterlee et al., 2019). On the other hand, accepting sedimentation in the polders increases the polder elevation and results over time in a wide and safe barrier between the land and estuary. The double dike system is then transformed into an alternative building with nature application.

Attenuation capacity

The effect of intertidal areas on a storm surge wave is shown in previous researches. Various studies focused on Saeftingen, a large intertidal area of 3500ha which lies 52km upstream in the Western Scheldt (Smolders, Plancke, Ides, Meire, & Temmerman, 2015). Attenuation rates due to this single intertidal area varies between 0.1-0.2m (Smolders et al., 2020; J. Stark, Smolders, Meire, & Temmerman, 2017). This research showed that 28 medium sized polders with a total area of 2240ha reduced a storm surge wave by 1.17m. The difference in results can be attributed to several factors. First, the storm surge wave height in this research was higher than in the other researches. The storage volume of the polders could be used to higher/full capacity. Secondly, in the model are the polders located at mean low water, which represents the initial situation well. To run future simulations polder elevation should be increased, without human interference it increases until mean high water. The intertidal area of Saeftingen reaches up to 3mNAP. So, while the area of Saeftingen is larger than the polders, the total storage volume is smaller than the polders in the model. Lastly, both Stark (2017) and Smolders (2020) used more complex models compared to this conceptual model. This simple model ignores several processes. However, the validation showed the ability of the model to predict the water level in the polders correctly.

The attenuation capacity of the double dike system increases upstream in the estuary. Similar results have been found in different model studies (Smolders et al., 2015; J. Stark et al., 2017). During the implementation of the Sigmaplan are several flood controlled areas (FCA) created upstream of Antwerp. The aim was to reduce the water level in the Scheldt during a storm surge. Smolders (2020) showed with a hindcast of 2013 storm that the FCAs reduced the maximal water level with 0.5m. A result with more closely resembles the attenuation capacity found in this research.

Creating a double dike system in an estuary increases the estuary volume, past research showed an increase in tidal prism when the estuary volume became larger (Coen, Peeters, & Mostaert, 2008). An increase in tidal prism could undo the effect of the added polders. However, more recent research indicated that tidal prism stayed constant or decreased for addition of extra intertidal areas (J. Stark et al., 2017). The double dike system does not increase the tidal prism.

Economic benefit

From a coastal protection viewpoint, the best solution would be to open all the available polders. Thereby creating the highest reduction in maximal water level and developing the largest field experiment so far. However, the implementation of this system is not solely limited by the physical feasibility.
The application of a double dike system has enormous implications of the inhabitations of Zeeland. Large parts of agricultural fields, villages and houses have to be displaced. The economic cost of land acquisition is valuable. In 2006 the Dutch government spend €285 million on 8600ha of land (van der Molen, 2015). The Dutch government has to compensate the owners fully for the expropriated land by law (Sluysmans, Verbist, & de Graaff, 2014). However, on the long-term is this

still the least expensive option. The Sigmaplan is a clear example, the implementation cost €600 million. However, calculations have shown that flood damage in 2100 could cost up to €1 billion per year (Temmerman et al., 2013). The creation of a double dike system gives besides flood safety also place for new uses (Dubbeldam, 2019). Wet agriculture, nature parks and recreation (i.e. beaches) may contribute to an enhanced economic value of this area. Also, the possibility of energy production in the inlet area of the polders may be of finical interest (appendix 16). Creating new nature areas, will increase the local biodiversity, which has a positive effect on the recreational experience (Marzetti Dall'aste Brandolini, 2006) and tourists appreciate the natural attractiveness (Petrosillo, Zurlini, Corliano, Zaccarelli, & Dadamo, 2007). The Perkpolder is a good example of how coastal safety can be increased and supporting the local social and economic value (Ginkel & Mooyaart, 2012). The project Perkpolder has a positive effect on the biodiversity, the population of benthos and birds are increasing. "The system is developing just a one would expect that a natural system would do" (Walles, Brummelhuis, van der Pool, Wiesebron, & Ysebaert, 2019). By being able to combine these factors, one could increase the incentive to invest in nature based coastal engineering. The implementation of a double dike system comes with an investment (e.g. acquisition cost, shifting to wet agriculture etc…). This can be earned back from increased activities in the region. Nevertheless, the main economic benefit is related to the prevention of flooding's in the future.

Public perception

The perception of the public may hinder the implementation; an example of a recent building with nature project. The Hedwige-Prosper project, this polder is given back to nature (Western Scheldt). The planning started in 2005, driven by the Natura 2000 legislation, to stop the reduction in the biodiversity. The aversion in Zeeland against non-conventional coastal defences caused the project to be slowed down. This aversion is mainly driven by the 1953 flood. The plan resulted in years of lawsuits and public protests to stop the realization, before the government finally could acquisition the land after 10 years. In 2018 started the ground acquisition and later the depoldering of the area could also start (*Rijksinpassingsplan Hertogin Hedwigepolder* 2014). The polder is still dry, the first water entering the polder is expected in 2022. On the other side of the spectrum is the Sandmotor project, which had a smooth implementation. One of the most important difference was the involvement of the public, which helped with the acceptance of the project (Vriend & Koningsveld, 2012). This research used the Western Scheldt as test case, to ensure possible implementation extremely careful communication to the public and media is important. It should be clear that coastal safety is always the priority during the development of a nature-based approach. Also, the increased economic benefit should be highlighted to increase acceptance. To convey this message is it crucial to give the public insight and a say in the final project, leaving them out only increases the aversion. In addition, the inclusion of many different stakeholders may help, this gives the possibility for each stakeholder profit from the project. If stakeholders can benefit from a project (e.g. tourism, creation of nature etc.), the willingness to participate is larger. From a scientific approach there is a need for a transdisciplinary approach, a holistic approach in which all fields are combined, to ensure best possible solution regarding suitability and innovation (Nesshöver et al., 2017).
So, when starting with a large-scale building with nature project it is of essence to involve the local population, stakeholders and scientist from all fields. The current delta plans for Zeeland show a need for innovative methods to safeguard the land. Almost the whole Western Scheldt is suitable for innovative dike enhancements (Deltacommissaris, 2014). In the Eastern Scheldt, projects concerning building with nature are stimulated (Slabbers, Brader, & Sorée, 2018), thereby creating the policy necessary to implement a double dike system. I would like to argue that the double dike system can be one of the potential methods suitable for this application. As there is already a policy that requires innovative solutions is a huge first step to promote and continue research on the application of building with nature in this region.

The possibilities of the developed model are not limited to storm surge attenuation of a double dike system. The model can be used to predict the tidal range in polders, information which essential to understand for the formation of salt marshes (Bouma et al., 2014; Zanuttigh et al., 2014). A double dike system can reduce a storm surge partly if it implemented on a large scale. Often new experiments are implemented on small scale to tests the capabilities, however, this will not result in a significant decrease of the estuary water level. Hence the importance to apply building with nature on a larger scale in the Western Scheldt, a double dike system will not be *the* solution, but it can certainly be part of one. The Western Scheldt test case provided useful insights; the findings can be applied to delta's globally. The model developed here can easily be applied for different estuaries by changing only a few parameters. Testing if a double dike system could apply to a specific estuary hasn't been easier. Creating insight and sharing knowledge could strengthen coastal defences worldwide. With hundreds of millions of lives at risk of flooding next century, it is essential to rethink our coastal defence strategy.

References

AHN. (2019). Actueel Hoogtebestand Nederland. Retrieved from https://www.ahn.nl/ahn-viewer

Baeyens, W., Van Eck, B., Lambert, C., Wollast, R., & Goeyens, L. (1998). General description of the Scheldt estuary *Trace Metals in the Westerschelde Estuary: A Case-Study of a Polluted, Partially Anoxic Estuary* (pp. 1-14): Springer.

Beniston, M., Stephenson, D. B., Christensen, O. B., Ferro, C. A., Frei, C., Goyette, S., . . . Koffi, B. (2007). Future extreme events in European climate: an exploration of regional climate model projections. *Climatic Change, 81*(1), 71-95.

Blum, M. D., & Roberts, H. H. (2009). Drowning of the Mississippi Delta due to insufficient sediment supply and global sea-level rise. *Nature Geoscience, 2*(7), 488-491. doi:10.1038/ngeo553

Bolle, A., Bing Wang, Z., Amos, C., & De Ronde, J. (2010). The influence of changes in tidal asymmetry on residual sediment transport in the Western Scheldt. *Continental Shelf Research, 30*(8), 871-882. doi:https://doi.org/10.1016/j.csr.2010.03.001

Borsje, B. W., van Wesenbeeck, B. K., Dekker, F., Paalvast, P., Bouma, T. J., van Katwijk, M. M., & de Vries, M. B. (2011). How ecological engineering can serve in coastal protection. *Ecological Engineering, 37*(2), 113-122.

Bouma, T. J., Van Belzen, J., Balke, T., Zhu, Z., Airoldi, L., Blight, A. J., . . . Hoggart, S. P. (2014). Identifying knowledge gaps hampering application of intertidal habitats in coastal protection: Opportunities & steps to take. *Coastal Engineering, 87*, 147-157.

Brière, C., Janssen, S. K., Oost, A. P., Taal, M., & Tonnon, P. K. (2018). Usability of the climate-resilient nature-based sand motor pilot, The Netherlands. *Journal of coastal conservation, 22*(3), 491-502.

Bujang, M. A., & Baharum, N. (2016). Sample size guideline for correlation analysis. *World Journal of Social Science Research, 3*(1).

Calkins, K. G. (2005). Power and Sample Size. Retrieved from http://www.andrews.edu/~calkins/math/edrm611/edrm11.htm

Callaghan, D. P., Bouma, T. J., Klaassen, P., van der Wal, D., Stive, M. J. F., & Herman, P. M. J. (2010). Hydrodynamic forcing on salt-marsh development: Distinguishing the relative importance of waves and tidal flows. *Estuarine, Coastal and Shelf Science, 89*(1), 73-88. doi:https://doi.org/10.1016/j.ecss.2010.05.013

Cheong, S.-M., Silliman, B., Wong, P. P., Van Wesenbeeck, B., Kim, C.-K., & Guannel, G. (2013). Coastal adaptation with ecological engineering. *Nature climate change, 3*(9), 787.

Coen, L., Peeters, P., & Mostaert, F. (2008). Inventarisatie en historische analyse Zeeschelde habitats: Effect antropogene ingrepen en natuurlijke evoluties op de getij-indringing in de Zeeschelde-Ondersteunende numerieke 1D-modellering. *WL Rapporten*.

Cox, T., Maris, T., De Vleeschauwer, P., De Mulder, T., Soetaert, K., & Meire, P. (2006). Flood control areas as an opportunity to restore estuarine habitat. *Ecological Engineering, 28*(1), 55-63. doi:https://doi.org/10.1016/j.ecoleng.2006.04.001

de Jong, D. J., & de Jonge, V. N. (1995). Dynamics and distribution of microphytobenthic chlorophyll-a in the Western Scheldt estuary (SW Netherlands). *Hydrobiologia, 311*(1), 21-30. doi:10.1007/bf00008568

de Vet, L., van Prooijen, B., & Wang, Z. B. (2019). *Towards a classification of the morphological development of intertidal flats: a comparison between the Eastern and Western Scheldt*. Retrieved from

Debernard, J. B., & Røed, L. P. (2008). Future wind, wave and storm surge climate in the Northern Seas: a revisit. *Tellus A: Dynamic Meteorology and Oceanography, 60*(3), 427-438.

Deltacommissaris. (2014). *Synthesedocument Zuidwestelijke Delta*. Retrieved from https://www.deltacommissaris.nl/binaries/deltacommissaris/documenten/publicaties/2014/09/16/deltaprogramma-2015-achtergronddocument-b8/DP2015+B8+Synthesedocument+Zuidwestelijke+Delta_tcm309-358059.pdf

Donat, M., Renggli, D., Wild, S., Alexander, L., Leckebusch, G., & Ulbrich, U. (2011). Reanalysis suggests long-term upward trends in European storminess since 1871. *Geophysical Research Letters, 38*(14).

Dong, Z., Wang, X., Zhao, A., Liu, L., & Liu, X. (2001). Aerodynamic roughness of fixed sandy beds. *Journal of Geophysical Research: Solid Earth, 106*(B6), 11001-11011.

Dubbeldam, T. (2019). Climate-Proofing The Coast of Zeeland

Ginkel, M. v., & Mooyaart, L. (2012). *Projectplan Aanpassing waterkering Perkpolder* Retrieved from Rotterdam: https://www.zeeweringenwiki.nl/images/2/2e/ProjectplanAanpassingWaterkeringPerkpolder.pdf

Google Earth. (2019). Google Earth Pro.

Hallegatte, S., Green, C., Nicholls, R. J., & Corfee-Morlot, J. (2013). Future flood losses in major coastal cities. *Nature climate change, 3*(9), 802-806. doi:10.1038/nclimate1979

Hinkel, J., Lincke, D., Vafeidis, A. T., Perrette, M., Nicholls, R. J., Tol, R. S. J., . . . Levermann, A. (2014). Coastal flood damage and adaptation costs under 21st century sea-level rise. *Proceedings of the National Academy of Sciences, 111*(9), 3292-3297. doi:10.1073/pnas.1222469111

Horstman, E. M., Dohmen-Janssen, C. M., Narra, P., Van den Berg, N., Siemerink, M., & Hulscher, S. J. (2014). Wave attenuation in mangroves: A quantitative approach to field observations. *Coastal Engineering, 94*, 47-62.

Huthnance, J. M. (1991). Physical oceanography of the North Sea. *Ocean and Shoreline Management, 16*(3), 199-231. doi:https://doi.org/10.1016/0951-8312(91)90005-M

Jacobs, S., Beauchard, O., Struyf, E., Cox, T., Maris, T., & Meire, P. (2009). Restoration of tidal freshwater vegetation using controlled reduced tide (CRT) along the Schelde Estuary (Belgium). *Estuarine, Coastal and Shelf Science, 85*(3), 368-376. doi:https://doi.org/10.1016/j.ecss.2009.09.004

Jentink, R. (2015). *Waterstandsmetingen Rammegors*. Retrieved from https://www.rijkswaterstaat.nl/

Jones, H. P., Hole, D. G., & Zavaleta, E. S. (2012). Harnessing nature to help people adapt to climate change. *Nature climate change, 2*(7), 504.

Kabat, P., Fresco, L. O., Stive, M. J., Veerman, C. P., Van Alphen, J. S., Parmet, B. W., . . . Katsman, C. A. (2009). Dutch coasts in transition. *Nature Geoscience, 2*(7), 450.

Kärnä, T., & Baptista, A. M. (2016). Evaluation of a long-term hindcast simulation for the Columbia River estuary. *Ocean Modelling, 99*, 1-14. doi:https://doi.org/10.1016/j.ocemod.2015.12.007

Kleinhans, M. G. (2005). Flow discharge and sediment transport models for estimating a minimum timescale of hydrological activity and channel and delta formation on Mars. *Journal of Geophysical Research: Planets, 110*(E12).

KNMI. (2019). Daggegevens van het weer in Nederland. Retrieved from https://www.knmi.nl/nederland-nu/klimatologie/daggegevens

Krauss, K. W., Doyle, T. W., Doyle, T. J., Swarzenski, C. M., From, A. S., Day, R. H., & Conner, W. H. (2009). Water level observations in mangrove swamps during two hurricanes in Florida. *Wetlands, 29*(1), 142.

LaMorte, W. W. (2016). Central Limit Theorem. *The Role of Probability.* Retrieved from http://sphweb.bumc.bu.edu/otlt/MPH-Modules/BS/BS704_Probability/BS704_Probability12.html

Leuven, J. R. F. W., Pierik, H. J., Vegt, M. v. d., Bouma, T. J., & Kleinhans, M. G. (2019). Sea-level-rise-induced threats depend on the size of tide-influenced estuaries worldwide. *Nature climate change*. doi:10.1038/s41558-019-0608-4

Maris, T., Cox, T., Temmerman, S., De Vleeschauwer, P., Van Damme, S., De Mulder, T., . . . Meire, P. (2007). Tuning the tide: creating ecological conditions for tidal marsh development in a flood control area. *Hydrobiologia, 588*(1), 31-43. doi:10.1007/s10750-007-0650-5

Marra, W. A., Braat, L., Baar, A. W., & Kleinhans, M. G. (2014). Valley formation by groundwater seepage, pressurized groundwater outbursts and crater-lake overflow in flume experiments with implications for Mars. *Icarus, 232*, 97-117.

Marzetti Dall'aste Brandolini, S. (2006). Investing in biodiversity: The recreational value of a natural coastal area. *Chemistry and Ecology, 22*(sup1), S443-S462.

McGranahan, G., Balk, D., & Anderson, B. (2007). The rising tide: assessing the risks of climate change and human settlements in low elevation coastal zones. *Environment and Urbanization, 19*(1), 17-37. doi:10.1177/0956247807076960

Möller, I., Kudella, M., Rupprecht, F., Spencer, T., Paul, M., Van Wesenbeeck, B. K., . . . Miranda-Lange, M. (2014). Wave attenuation over coastal salt marshes under storm surge conditions. *Nature Geoscience, 7*(10), 727.

Morris, R. L., Konlechner, T. M., Ghisalberti, M., & Swearer, Stephen E. (2018). From grey to green: Efficacy of eco-engineering solutions for nature-based coastal defence. *Global Change Biology, 24*(5), 1827-1842. doi:10.1111/gcb.14063

Morvan, H., Knight, D., Wright, N., Tang, X., & Crossley, A. (2008). The concept of roughness in fluvial hydraulics and its formulation in 1D, 2D and 3D numerical simulation models. *Journal of Hydraulic Research, 46*(2), 191-208.

Narayan, S., Beck, M. W., Reguero, B. G., Losada, I. J., van Wesenbeeck, B., Pontee, N., . . . Burks-Copes, K. A. (2016). The Effectiveness, Costs and Coastal Protection Benefits of Natural and Nature-Based Defences. *PLOS ONE, 11*(5), e0154735. doi:10.1371/journal.pone.0154735

Nasir, B. A. (2013). Design of high efficiency cross-flow turbine for hydro-power plant. *International Journal of Engineering and Advanced Technology (IJEAT) ISSN*, 2249-8958.

Nasir, B. A. (2014). Design Considerations of Micro-hydro-electric Power Plant. *Energy Procedia, 50*, 19-29. doi:https://doi.org/10.1016/j.egypro.2014.06.003

Neill, S. P., & Hashemi, M. R. (2018). Chapter 10 - Other Aspects of Ocean Renewable Energy. In S. P. Neill & M. R. Hashemi (Eds.), *Fundamentals of Ocean Renewable Energy* (pp. 271-309): Academic Press.

Nesshöver, C., Assmuth, T., Irvine, K. N., Rusch, G. M., Waylen, K. A., Delbaere, B., . . . Wittmer, H. (2017). The science, policy and practice of nature-based solutions: An interdisciplinary perspective. *Science of The Total Environment, 579*, 1215-1227. doi:https://doi.org/10.1016/j.scitotenv.2016.11.106

Nguyen, A. D. (2008). *Salt Intrusion, Tides and Mixing in Multi-Channel Estuaries: PhD: UNESCO-IHE Institute, Delft.* CRC Press, Delft.

Nicholls, R. J., Hanson, S., Herweijer, C., Patmore, N., Hallegatte, S., Corfee-Morlot, J., . . . Muir-Wood, R. (2007). *Ranking of the World's Cities Most Exposed to Coastal Flooding Today and in the Future: Executive Summary*. Retrieved from Paris: https://climate-adapt.eea.europa.eu/metadata/publications/ranking-of-the-worlds-cities-to-coastal-flooding/11240357

Ofori, K., van der Wegen, M., Roelvink, J., & de Ronde, J. (2019). Investigating the trends of import and export of sediment in the Western Scheldt estuary, The Netherlands—by a process-based model. *River, Coastal and Estuarine Morphodynamics. RCEM 2009, 2*, 229-236.

Oosterlee, L., Cox, T. J. S., Temmerman, S., & Meire, P. (2019). Effects of tidal re-introduction design on sedimentation rates in previously embanked tidal marshes. *Estuarine, Coastal and Shelf Science*, 106428. doi:https://doi.org/10.1016/j.ecss.2019.106428

Ott, R. L., & Longnecker, M. T. (2015). *An introduction to statistical methods and data analysis* (6th ed.): Nelson Education.

Oxford English Dictionary. (2019). Oxford English Dictionary. Retrieved from https://www.oed.com/

Petrosillo, I., Zurlini, G., Corliano, M., Zaccarelli, N., & Dadamo, M. (2007). Tourist perception of recreational environment and management in a marine protected area. *Landscape and urban planning, 79*(1), 29-37.

Pörtner, H.-O., Roberts, D. C., Masson-Delmotte, V., Zhai, P., Tignor, M., Poloczanska, E., . . . (eds.), N. W. (2019). *Summary for Policymakers. In: IPCC Special Report on the Ocean and Cryosphere in a Changing Climate* Retrieved from

Python. (2019). Python Software Foundation (Version 3.7.x). Retrieved from http://www.python.org

Rijksinpassingsplan Hertogin Hedwigepolder (2014). Retrieved from Ministerie Economische Zaken & Ministerie Infrastructuur & Milieu

Rijkswaterstaat. (2019). Rijkswaterstaat Waterinfo. Retrieved from https://waterinfo.rws.nl/

Roode, N. (2008). *Risks, safety standards and probabilistic techniques in five countries along the North Sea*.

Rouse, H. (1965). Critical Analysis of Open-Channel Resistance. *Journal of the Hydraulics Division, 91*(4), 1-23.

Schmidt, C. (2015). Alarm over a sinking delta. *Science, 348*(6237), 845-846. doi:10.1126/science.348.6237.845

Schmidt, C. W. (2015). Delta Subsidence: An Imminent Threat to Coastal Populations. *Environmental Health Perspectives, 123*(8), A204-A209. doi:doi:10.1289/ehp.123-A204

Shepard, C. C., Crain, C. M., & Beck, M. W. (2011). The protective role of coastal marshes: a systematic review and meta-analysis. *PLOS ONE, 6*(11), e27374.

Sistermans, P., & Nieuwenhuis, O. (2004). *Western Scheldt estuary (the Netherlands)*. Retrieved from Amersfoort: http://copranet.projects.eucc-d.de/files/000142_EUROSION_Western_Scheldt.pdf

Slabbers, S., Brader, R., & Sorée, C. (2018). *Oosterscheldevisie 2018-2024*. Retrieved from https://www.zeeland.nl/digitaalarchief/zee1800091

Sluysmans, J., Verbist, S., & de Graaff, R. (2014). Compensation for Expropriation: How Compensation Reflects a Vision on Property *European Property Law Journal* (Vol. 3, pp. 3).

Smolders, S., João Teles, M., Leroy, A., Maximova, T., Meire, P., & Temmerman, S. (2020). Modeling Storm Surge Attenuation by an Integrated Nature-Based and Engineered Flood Defense System in the Scheldt Estuary (Belgium). *Journal of Marine Science and Engineering, 8*(1), 27.

Smolders, S., Plancke, Y., Ides, S., Meire, P., & Temmerman, S. (2015). Role of intertidal wetlands for tidal and storm tide attenuation along a confined estuary: a model study. *Natural hazards and earth systems sciences.--, 15*(7), 1659-1675.

SPSS. (2017). IBM SPSS Statistics for Windows (Version 25.0). NY IBM Corp.

Stark, J., Plancke, Y., Ides, S., Meire, P., & Temmerman, S. (2016). Coastal flood protection by a combined nature-based and engineering approach: Modeling the effects of marsh geometry and surrounding dikes. *Estuarine, Coastal and Shelf Science, 175*, 34-45. doi:https://doi.org/10.1016/j.ecss.2016.03.027

Stark, J., Smolders, S., Meire, P., & Temmerman, S. (2017). Impact of intertidal area characteristics on estuarine tidal hydrodynamics: A modelling study for the Scheldt Estuary. *Estuarine, Coastal and Shelf Science, 198*, 138-155. doi:https://doi.org/10.1016/j.ecss.2017.09.004

Stark, J., Smolders, S., & Vandenbruwaene, W. (2019). *Using Numerical Simulations to Improve Insight on the Historical Evolution of Tides And Morphology in the Scheldt Estuary*.

Stark, J., Van Oyen, T., Meire, P., & Temmerman, S. (2015). Observations of tidal and storm surge attenuation in a large tidal marsh. *Limnology and Oceanography, 60*(4), 1371-1381.

Sterl, A., van den Brink, H., Haarsma, R., de Vries, H., & van Meijgaard, E. (2009). Stormklimaat en hoogwaters. *Meteorologica, 2*, 10-11.

Streeter, V. L., & Wylie, E. B. (1985). *Fluid mechanics*. New York: McGraw-Hill.

Tangelder, M., Troost, K., van den Ende, D., & Ysebaert, T. (2012). *Biodiversity in a changing Oosterschelde: from past to present*. Retrieved from

Taylor, K. E. (2001). Summarizing multiple aspects of model performance in a single diagram. *Journal of Geophysical Research: Atmospheres, 106*(D7), 7183-7192.

Temmerman, S., & Kirwan, M. L. (2015). Building land with a rising sea. *Science, 349*(6248), 588-589. doi:10.1126/science.aac8312

Temmerman, S., Meire, P., Bouma, T., Herman, P., Ysebaert, T., & de Vriend, H. (2013). Ecosystem-based coastal defence in the face of global change. *Nature, 504*, 79-83. doi:10.1038/nature12859

van der Molen, P. (2015). Property and administration: Comparative observations on property rights and spatial planning with some cases from the Netherlands. *Administration & society, 47*(2), 171-196.

Van Rijn, L. (2010). Tidal phenomena in the Scheldt Estuary. *Report, Deltares, 105*, 99.

Van Slobbe, E., de Vriend, H. J., Aarninkhof, S., Lulofs, K., de Vries, M., & Dircke, P. (2013). Building with Nature: in search of resilient storm surge protection strategies. *Natural hazards, 66*(3), 1461-1480.

van Wesenbeeck, B. K., Mulder, J. P., Marchand, M., Reed, D. J., de Vries, M. B., de Vriend, H. J., & Herman, P. M. (2014). Damming deltas: a practice of the past? Towards nature-based flood defenses. *Estuarine, Coastal and Shelf Science, 140*, 1-6.

Vousdoukas, M. I., Voukouvalas, E., Annunziato, A., Giardino, A., & Feyen, L. (2016). Projections of extreme storm surge levels along Europe. *Climate Dynamics, 47*(9), 3171-3190. doi:10.1007/s00382-016-3019-5

Vriend, H. d., & Koningsveld, M. v. (2012). *Building with Nature: Thinking, acting and interacting differently* (V. Jones Ed.): EcoShape, Building with Nature.

Walles, B., Brummelhuis, E., van der Pool, J., Wiesebron, L., & Ysebaert, T. (2019). *Development of benthos and birds in an intertidal area created for coastal defence (Scheldt estuary, the Netherlands)*. Retrieved from

Wang, Z., Jeuken, M., Gerritsen, H., De Vriend, H., & Kornman, B. (2002). Morphology and asymmetry of the vertical tide in the Westerschelde estuary. *Continental Shelf Research, 22*(17), 2599-2609.

Weisse, R., von Storch, H., Niemeyer, H. D., & Knaack, H. (2012). Changing North Sea storm surge climate: an increasing hazard? *Ocean & Coastal Management, 68*, 58-68.

Woth, K., Weisse, R., & von Storch, H. (2006). Climate change and North Sea storm surge extremes: an ensemble study of storm surge extremes expected in a changed climate projected by four different regional climate models. *Ocean Dynamics, 56*(1), 3-15. doi:10.1007/s10236-005-0024-3

Yang, H. F., Yang, S. L., Xu, K. H., Wu, H., Shi, B. W., Zhu, Q., . . . Yang, Z. (2017). Erosion potential of the Yangtze Delta under sediment starvation and climate change. *Scientific Reports, 7*(1), 10535. doi:10.1038/s41598-017-10958-y

Zanuttigh, B., Losada, I. J., Nicholls, R. J., Thompson, R. C., Vanderlinden, J.-P., & Burcharth, H. F. (2014). *Coastal Risk Assessment and Mitigation in a Changing Climate*. Oxford, UNITED STATES: Elsevier Science & Technology.

Zeghadnia, L., Robert, J. L., & Achour, B. (2019). Explicit solutions for turbulent flow friction factor: A review, assessment and approaches classification. *Ain Shams Engineering Journal, 10*(1), 243-252. doi:https://doi.org/10.1016/j.asej.2018.10.007

Zhou, J., Bao, W., Li, Y., Cheng, L., & Bao, M. (2018). The Modified One-Dimensional Hydrodynamic Model Based on the Extended Chezy Formula. *Water, 10*(12), 1743.

Zwolsman, J. J. G., Berger, G. W., & Van Eck, G. T. M. (1993). Sediment accumulation rates, historical input, postdepositional mobility and retention of major elements and trace metals in salt marsh sediments of the Scheldt estuary, SW Netherlands. *Marine Chemistry, 44*(1), 73-94. doi:https://doi.org/10.1016/0304-4203(93)90007-B

Appendix

Appendix 1: Variables

Variable	Name	Value*	Unit	Variable	Name	Value*	Unit
A	Amplitude	5.90	m	**Q**	Discharge		m^3min^{-1}
A_i	Inlet Area		m^2	**Q_s**	Discharge into the small Polder		m^3min^{-1}
A_p	Polder Area		m^2	**Q_m**	Discharge into the medium Polder		m^3min^{-1}
b	Offset	0	m	**Q_l**	Discharge into the large Polder		m^3min^{-1}
C	Chezy constant		1/η	**S**	Slope		m/m
f	Friction		-	**t**	Time	0-1250	minutes
f_m	Scaling factor water volume (Mid)	0.0035	-	**u**	Flow Velocity		ms^{-1}
f_{up}	Scaling factor water volume (Up)	0.006	-	**V_e**	Estuary Volume		m^3
g	Gravity Constant		ms^{-2}	**Vp**	Polder Volume		m^3
h	Sea Water Level from Mean Low Water		m	**w_e**	Width of the Western Scheldt		m
h_{max}	Maximal Water level		m	**w_i**	Inlet Width		m
h_p	Polder Water Level		m	**x**	Polder Width		m
k_s	Nikuradse Roughness Length	0.005	m	**x_d**	Dike Width	20	m
L	Length section Western Scheldt		m				
n	Number of data points		-	**y**	Polder Length		m
η	Manning coefficient		ms^{-1}	**z**	Dike Height	10	m
p	Period		min	**z_s**	Secondary Dike Height	6m (+NAP)	m
p_a				**z_0**	Height of diver above NAP		m
p_l	Number of Large sized Polders		-				
p_m	Number of Medium sized Polders		-				
p_s	Number of Small sized Polders		-				

*Values are only given for the variables that are constant.

Appendix 2: Top view double dike system

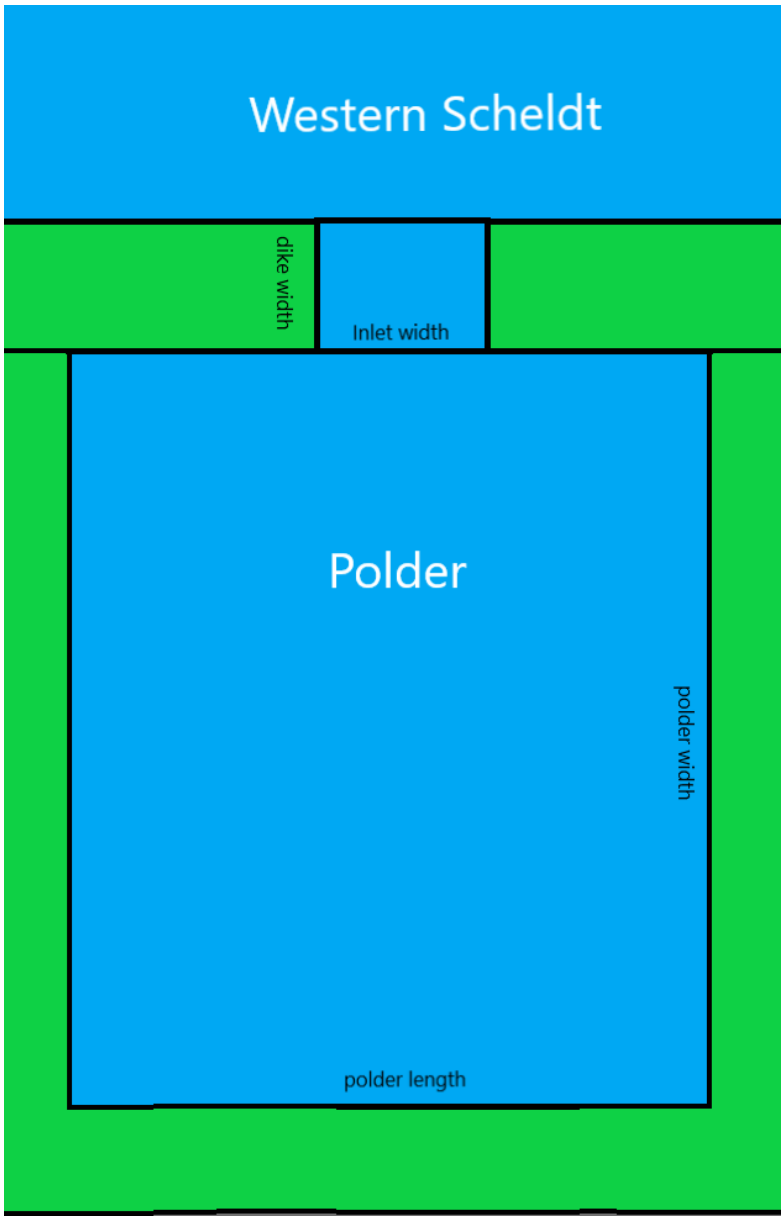

Figure A1 Sketch top view double dike system; dike width (d_w), inlet width (w_i), polder width (x) and length (y).

Appendix 3: Tests of Normality in SPSS for the polders of the Western Scheldt

Tests of Normality						
	Kolmogorov-Smirnov[a]			Shapiro-Wilk		
	Statistic	df	Sig.	Statistic	df	Sig.
Log(Area_ws)	0.091	57	0.200*	0.969	57	0.145

*. This is a lower bound of the true significance.

a. Lilliefors Significance Correction

Appendix 4: Main script Mid-Western Scheldt

```
"""
Simulating a double dike system upstream in the Western Scheldt
@author: Kasper de Vaan
"""
import numpy as np
import matplotlib.pyplot as plt
import math
fu = 0.541/6 #SCALING FACTOR
area_up = 42000000*fu#Area of mid-section Westerschelde multiplied with the factor to come to the correct volume
inlet = int(input("set inlet area [m2] (default = 60): ") or 60)
t1 = int(input("set simuation time [min] (default = 1250): ") or 1250)
a_ss = 5.90*1.4 #amplitude storm surge + amplification funneling
A_L = (1100*1000) # Area large polder
A_M = (800*1000) # Area Medium polder
A_S = (560*1000)# Area Small polder
nol= int(input("set number of large polders (default = 0): ") or 0)
nom= int(input("set number of medium polders (default = 0): ") or 0)
nos= int(input("set number of small polders  (default = 0): ") or 0)
dw = 20 #Dike width, used for the slope calculationg
dh = 10# dike height
time=np.arange(0,t1,1)
g = 9.81
f = 0.35
b_ss = 0
period_s = 2500 #Period storm surge
a = 1.765 #Amplitude storm surge
b = 0.295+(a-0.295) #take the mean low water
period = 12.4166*60 #semi-dirunal tide
def storm_tide (time):
    if (a_ss*math.sin((math.pi*2/period_s)*time)+b_ss) > 0 and t < period_s:
        h = ((a_ss*math.sin((math.pi*2/period_s)*time)+b_ss) + (a*math.sin((math.pi*2/period)*time)+b))
    else:
        h = (a*math.sin((math.pi*2/period)*time)+b)
    return h
def discharge (h, hp):
    if h == hp:
        S = 0
        dis = 0
    else:
        S = (h-hp)/dw
        C = math.sqrt((8*g)/f)
        if S > 0:
            u = C*(math.sqrt(dh*S))
            dis = u*inlet*60
        else:
            u = C*(math.sqrt(dh*S*-1))
            dis = u*inlet*60*-1
    return dis
wle_up = []  #water level Western Scheldt
LL=[]      #Large polder water Level
LS=[]      #Small polder water Level
LM=[]      #Medium polder water Level
vol_up = []  #Water Volume Estuary MID
ratio=[]    #Vp/Vws
ph_L = 0    #Polder Water level Large
ph_M = 0    #Polder Water level Medium
ph_S = 0    #Polder Water level Small
temp=[]
zs=[]
zm=[]
zl=[]
```

```
head=[]
dis=[]
h=storm_tide(0)
tot_Q=0
for t in time:
   Vmid = (storm_tide(t)*area_up)-tot_Q
   Q_L = discharge(h, ph_L)
   Q_M = discharge(h, ph_M)
   Q_S = discharge(h, ph_S)
   tot_Q = (Q_L*nol)+(Q_M*nom)+(Q_S*nos)
   head.append(h-ph_M)
   dis.append(Q_M)
   h=(Vmid/area_up)
   if nol == 0:
      ph_L = 0
   else:
      ph_L += (Q_L/(A_L*nol))
   if nom == 0:
      ph_M = 0
   else:
      ph_M += (Q_M/(A_M*nom))
   if nos == 0:
      ph_S = 0
   else:
      ph_S += (Q_S/(A_S*nos))
   vol_up.append(Vmid)
   polder_vol =  nol*A_L+nom*A_M+nos*A_S
   temp.append(polder_vol)
   wle_up.append(h)
   ratio.append(polder_vol/Vmid)   #volume polder/ volume Westerschelde
   LL.append(ph_L)              #Large polder water Level
   LM.append(ph_M)
   LS.append(ph_S)


plt.figure()
plt.plot(time, wle_up)
plt.title('Upstream Western Scheldt')
plt.xlabel("Time [min]")
plt.ylabel("Water level [m]")
plt.grid(True)

plt.figure()
plt.plot(time, LL, '-r', label="large")
plt.plot(time, LM, '-b', label="medium")
plt.plot(time, LS, '-k', label="small")
plt.xlabel("Time [min]")
plt.legend(loc='upper right')
plt.ylabel("Water level Polder [m]")
plt.grid(True)
sf = input(("Save figure? (y/n) ") or n)
print("...")
if sf == "y":
   np.savetxt("figure.png")

ini = 10.116
ac = (ini-max(wle_up))/ini*100
print("...")
print("Number of large polders", nol)
print("Number of medium polders", nom)
print("Number of small polders", nos)
print("Maximium water level Western Scheldt(Up) = ",round(max(wle_up),3) ,"mNAP")
print("Attenuation Capacity", round(ac,2),"%")
```

Appendix 5: Main script Upstream Western Scheldt

```
"""
Simulating a double dike system upstream in the Western Scheldt
@author: Kasper de Vaan
"""
import numpy as np
import matplotlib.pyplot as plt
import math
fm = 2.01/23          #SCALING FACTOR
area_m = 144000000*fm   #Area of mid-section Westerschelde multiplied with the factor to come to the correct volume
inlet = int(input("set inlet area [m2] (default = 60): ") or 60)
t2 = int(input("set simuation time [min] (default = 1250): ") or 1250)
a_ss = int(5.90*1.1)     #amplitude storm surge + amplification funneling
A_L = (1100*1000)       #Area large polder
A_M = (800*1000)        #Area Medium polder
A_S = (560*1000)        #Area Small polder
nol= int(input("set number of large polders (default = 0): ") or 0)
nom= int(input("set number of medium polders (default = 0): ") or 0)
nos= int(input("set number of small polders  (default = 0): ") or 0)
dw = 25               #Dike width, used for the slope calculationg
dh = 10               #Dike height, above mean low water
time=np.arange(0,t2,1)
g = 9.81
f = 0.35
ks = 0.005
b_ss = 0
period_s = 2500     #Period storm surge
a = int(1.765)          #Amplitude storm surge
b = int(0.295+(a-0.295)) #taking mean low water as reference
period = 12.4166*60 #semi-dirunal tide
def storm_tide (time):
    if (a_ss*math.sin((math.pi*2/period_s)*time)+b_ss) > 0 and t < period_s:
        h = ((a_ss*math.sin((math.pi*2/period_s)*time)+b_ss) + (a*math.sin((math.pi*2/period)*time)+b))
    else:
        h = (a*math.sin((math.pi*2/period)*time)+b)
    return h
def discharge (h, hp):
    if h == hp:
        S = 0
        dis = 0
    else:
        S = (h-hp)/dw
        C = math.sqrt((8*g)/f)
        if S > 0:
            u = C*(math.sqrt(dh*S))
            dis = u*inlet*60
        else:
            u = C*(math.sqrt(dh*S*-1))
            dis = u*inlet*60*-1
    return dis
wle_m = []  #water level Western Scheldt
LL=[]       #Large polder water Level
LS=[]       #Small polder water Level
LM=[]       #Medium polder water Level
vol_m = []  #Water Volume Estuary MID
ratio=[]    #Vp/Vws
ph_L = 0    #Polder Water level Large
ph_M = 0    #Polder Water level Medium
ph_S = 0    #Polder Water level Small
temp=[]
zs=[]
zm=[]
```

SCAN ME

```
zl=[]
hh=1
h=storm_tide(0)
tot_Q=0
for t in time:
    Vmid = (storm_tide(t)*area_m)-tot_Q
    Q_L = discharge(h, ph_L)
    Q_M = discharge(h, ph_M)
    Q_S = discharge(h, ph_S)
    tot_Q = (Q_L*nol)+(Q_M*nom)+(Q_S*nos)
    h=(Vmid/area_m)
    if nol == 0:
        ph_L = 0
    else:
        ph_L += (Q_L/(A_L*nol))
    if nom == 0:
        ph_M = 0
    else:
        ph_M += (Q_M/(A_M*nom))
    if nos == 0:
        ph_S = 0
    else:
        ph_S += (Q_S/(A_S*nos))
    vol_m.append(Vmid)
    polder_vol =  nol*A_L+nom*A_M+nos*A_S
    temp.append(polder_vol)
    wle_m.append(h)
    ratio.append(polder_vol/Vmid)   #volume polder/ volume Westerschelde
    LL.append(ph_L)               #Large polder water Level
    LM.append(ph_M)
    LS.append(ph_S)

plt.figure()
plt.plot(time, wle_m)
plt.title('Mid Estuary')
plt.xlabel("Time [min]")
plt.ylabel("Water level estuary [mMLW]")
plt.grid(True)

plt.figure()
plt.plot(time, LL, '-r', label="large")
plt.plot(time, LM, '-b', label="medium")
plt.plot(time, LS, '-k', label="small")
plt.legend(loc='upper right')
plt.ylabel("Water level estuary [mMLW]")
plt.grid(True)
sf = input(("Save figure? (y/n) ") or n)
print("...")
if sf == "y":
    np.savetxt("figure.png")
ini = 6.886
ac = (ini-max(wle_m))/ini*100
print("...")
print("Number of large polders", nol)
print("Number of medium polders", nom)
print("Number of small polders", nos)
print("Maximium water level Western Scheldt(Mid) = ",round(max(wle_m),3) ,"mNAP")
print("Attenuation Capacity", round(ac,2),"%")
```

Appendix 6: Roughness length sensitivity test

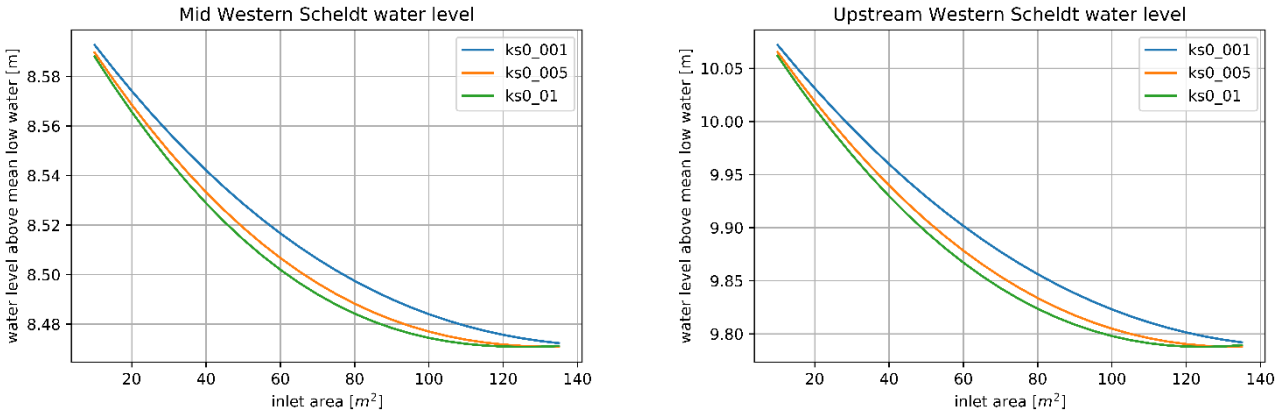

Figure A2 Water level in the (a) mid and (b) upstream Western Scheldt for a varying inlet area and k_s value

Descriptive Statistics - SPSS						
Midstream	N	Minimum	Maximum	Mean	Std. Deviation	Variance
Mid_ks01	38	8.47	8.59	8.4948	.03340	.001
Mid_ks005	38	8.47	8.59	8.4966	.03458	.001
Mid_ks001	38	8.47	8.59	8.5008	.03678	.001
Valid N (listwise)	38					

Descriptive Statistics - SPSS						
Upstream	N	Minimum	Maximum	Mean	Std. Deviation	Variance
Up_ks01	38	9.79	10.01	9.8487	.07020	.005
Up_ks005	38	9.79	10.01	9.8504	.07316	.005
Up_ks001	38	9.79	10.01	9.8575	.07791	.006
Valid N (listwise)	38					

Appendix 7: Calibration plots Rammegors and Perkpolder

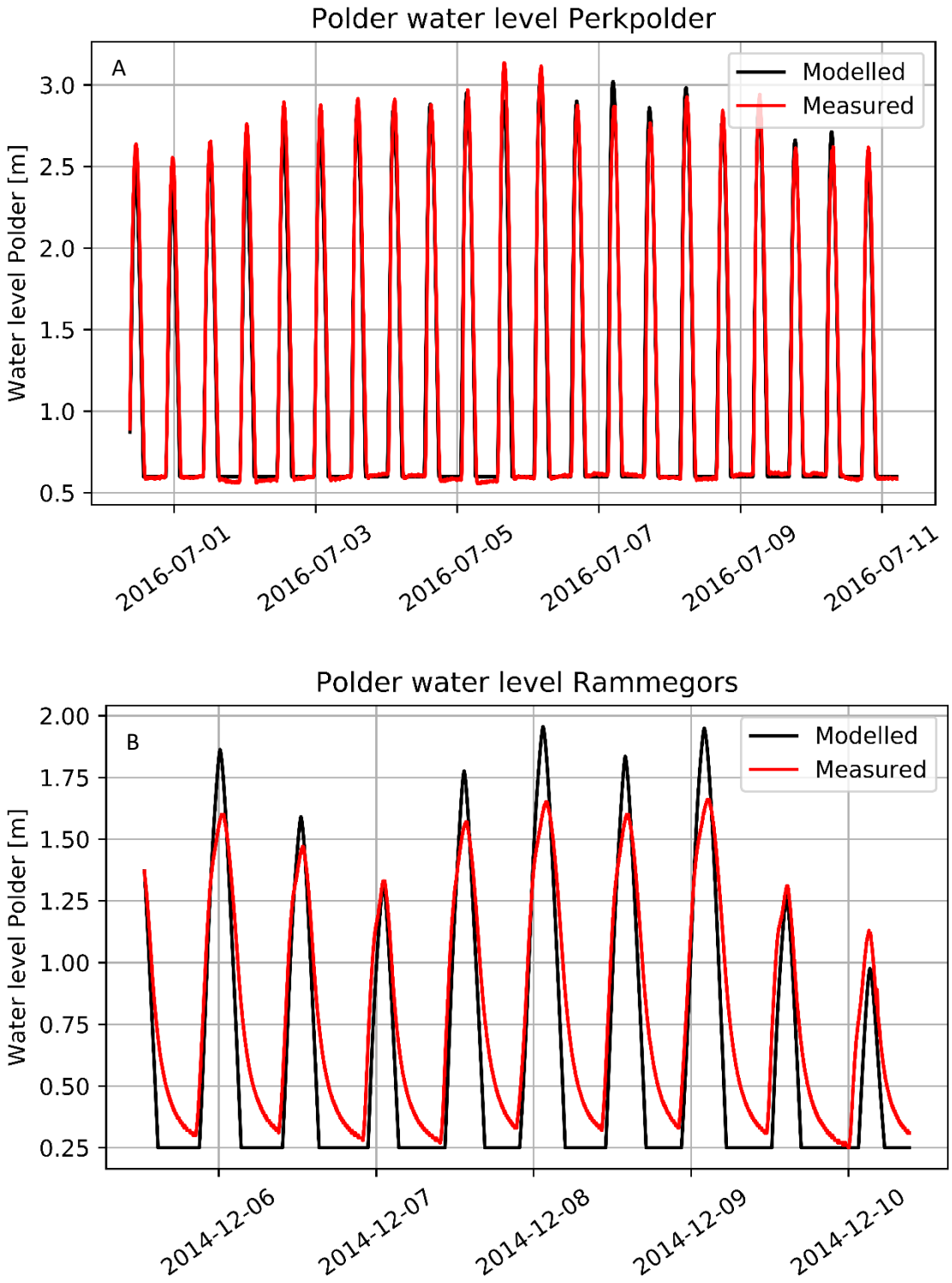

Figure A3 Modelled and Measured water levels in the (a) Perkpolder and (b) Rammegors for the calibration

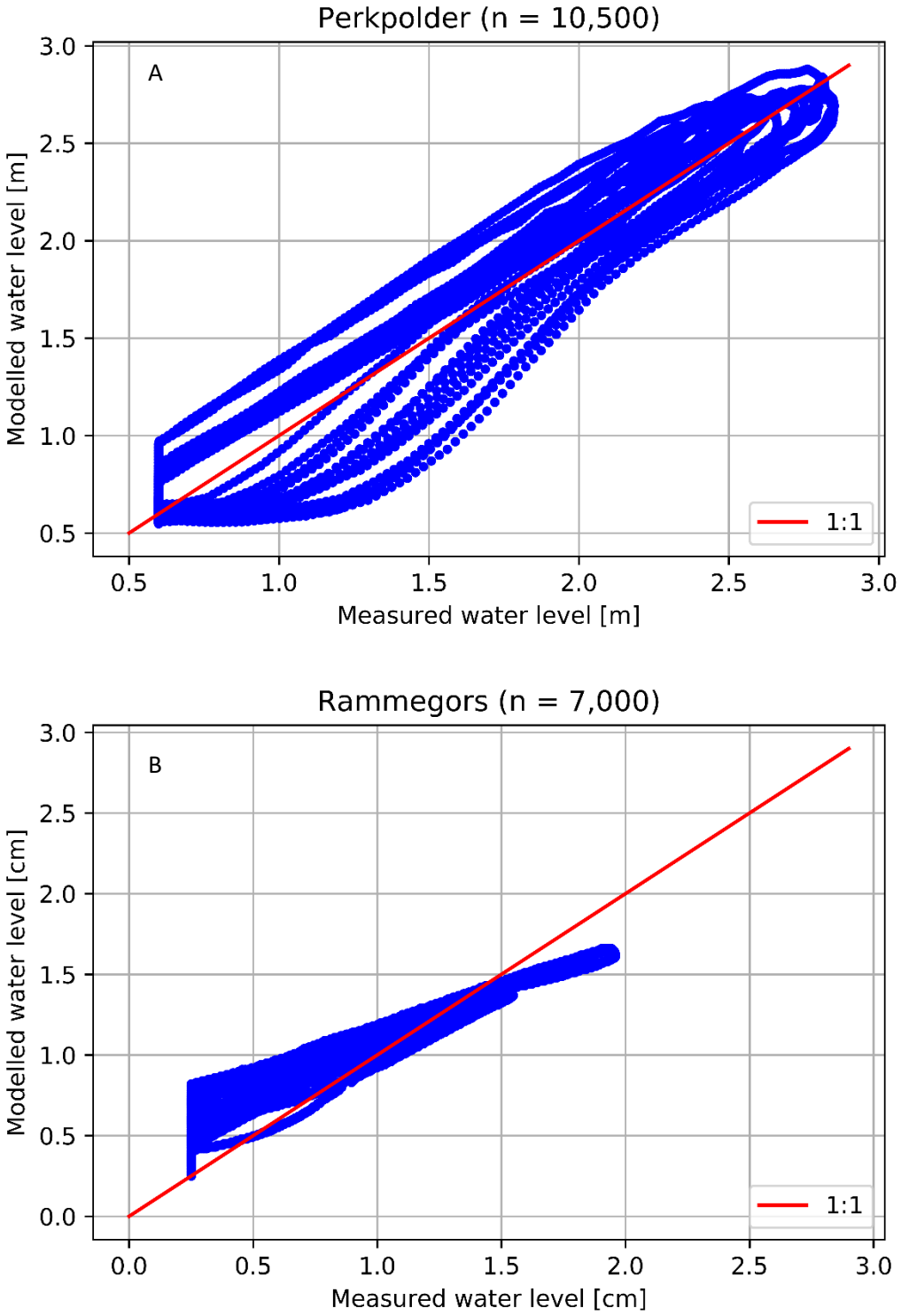

Figure A4 (a) Perkpolder and (b) Rammegors modelled and measured water levels, the red line is a 1:1-line indicting a perfect fit

Appendix 8: Elevation Map Rammegors polder

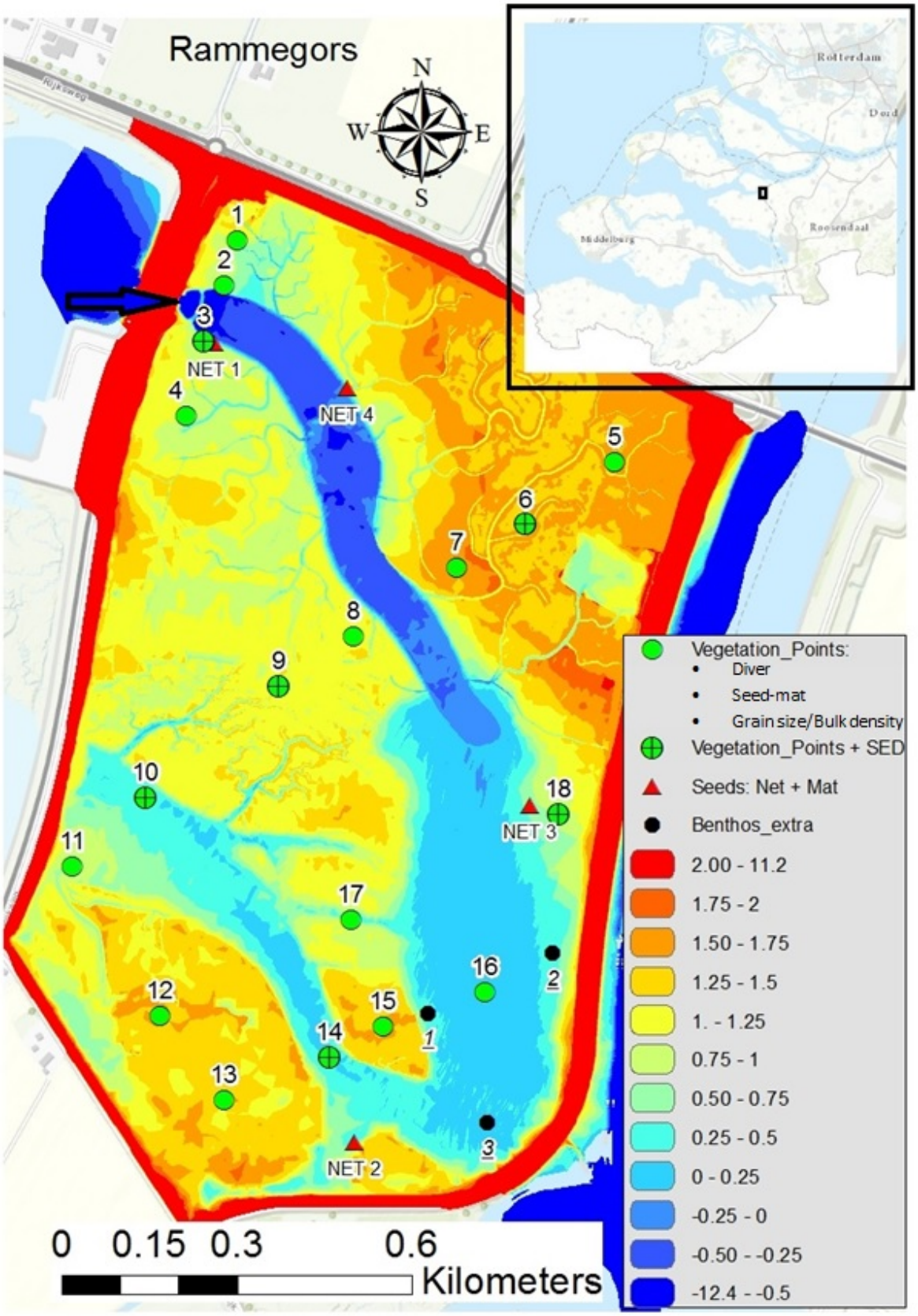

Figure A5 Rammegors elevation map, green dots indicate the location of the divers

Appendix 9: Elevation Map Perkpolder

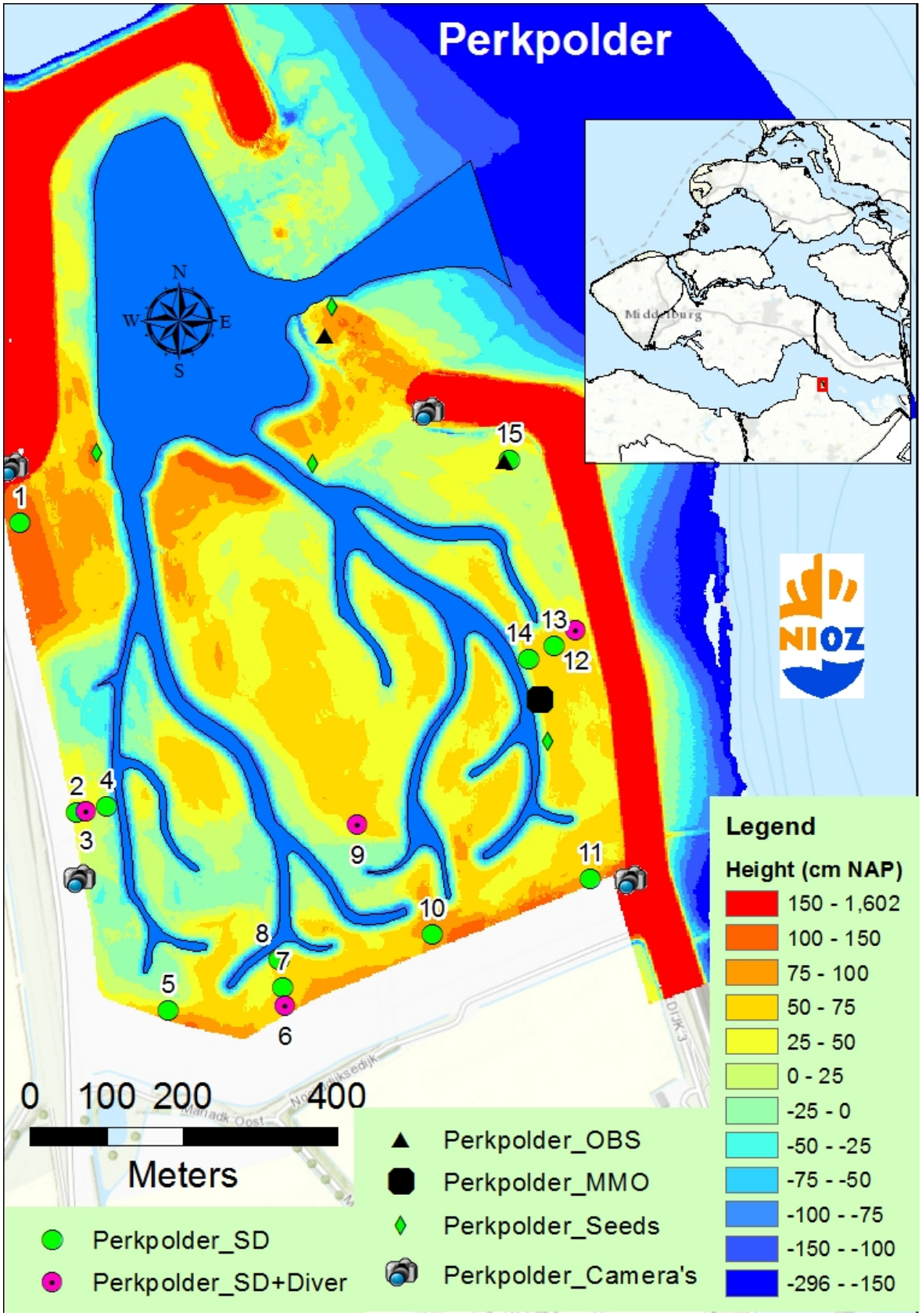

Figure A6 Perkpolder elevation map, pink dots indicate the location of the divers

Appendix 10: Timeseries measured and modelled water levels (Validation)

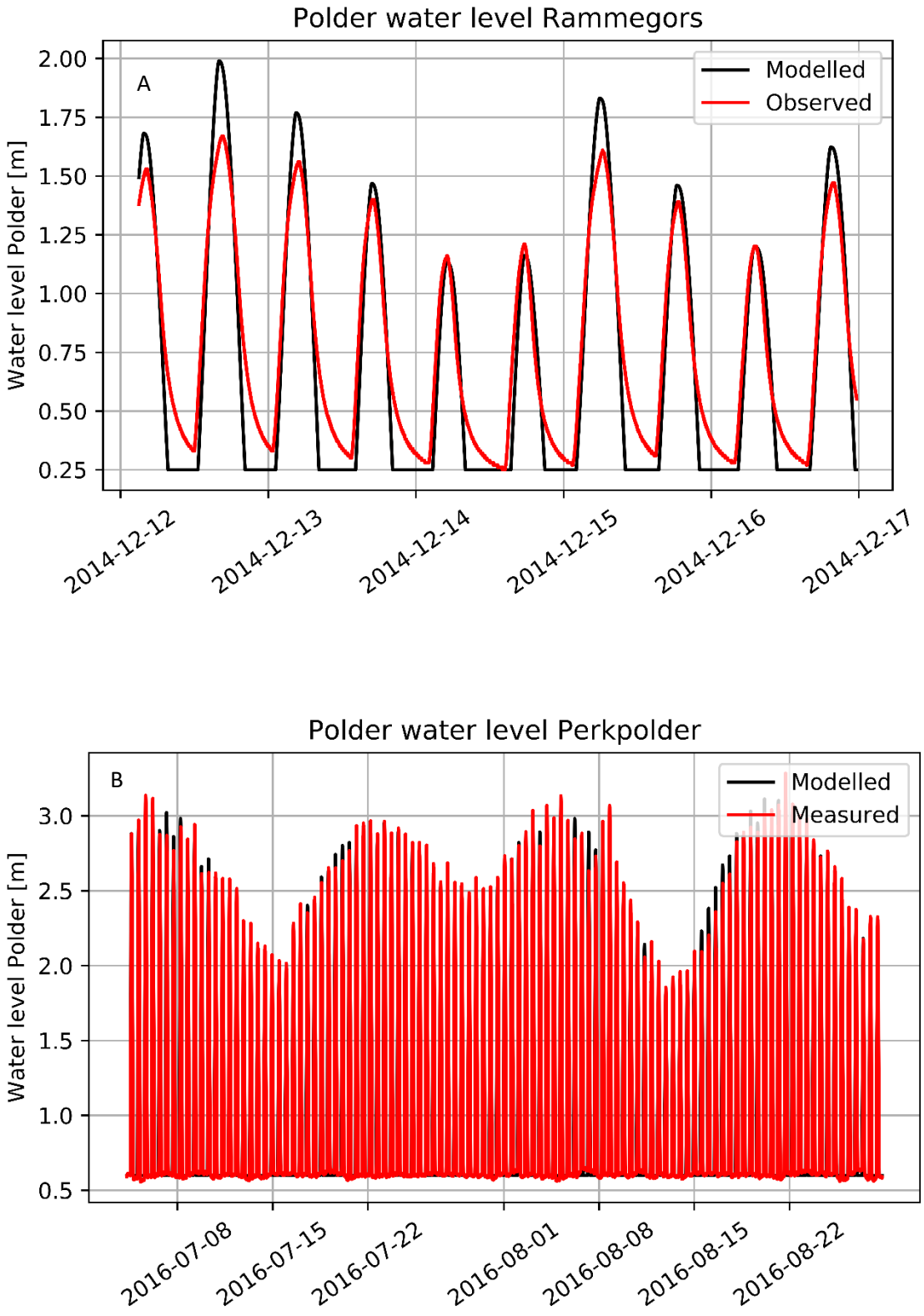

Figure A7 Modelled and Measured water levels in the (b) Perkpolder and (a) Rammegors for the calibration

Appendix 11: Simulation of a tidal wave

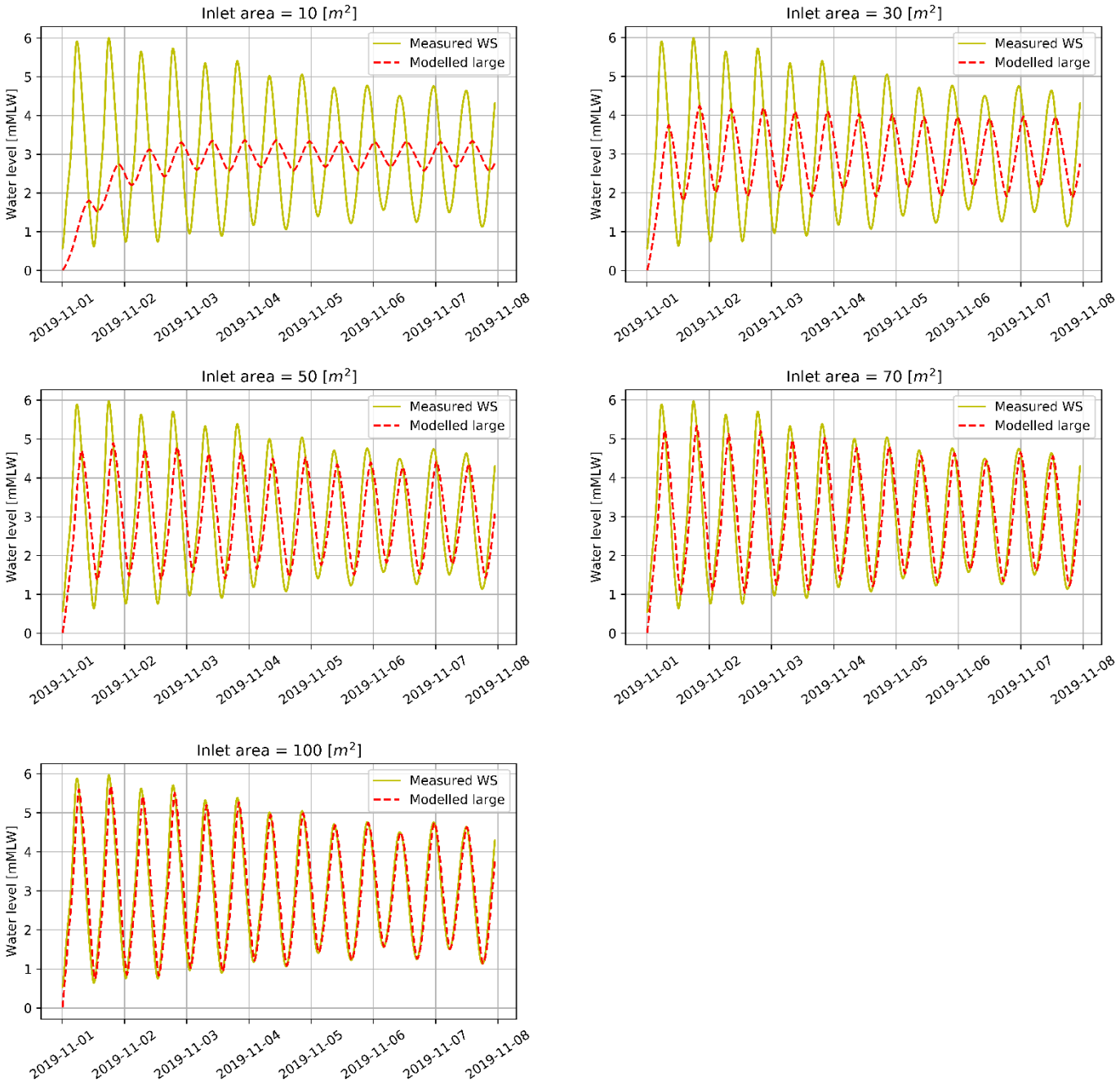

Figure A8 Modelled water levels in the polders and Western Scheldt for a normal tidal wave near Bath. As input is the estuary water level measurements used from Bath (Rijkswaterstaat, 2019).The solid yellow line indicates the measured water level in the Western Scheldt, water level relative to mean low water. The red dotted line indicates the modelled polder water level for a large polder with a varying inlet area. The tidal amplitude in the polders is reduced compared to the estuary. Further, the tidal amplitude in the polders depends on the size of the polder.

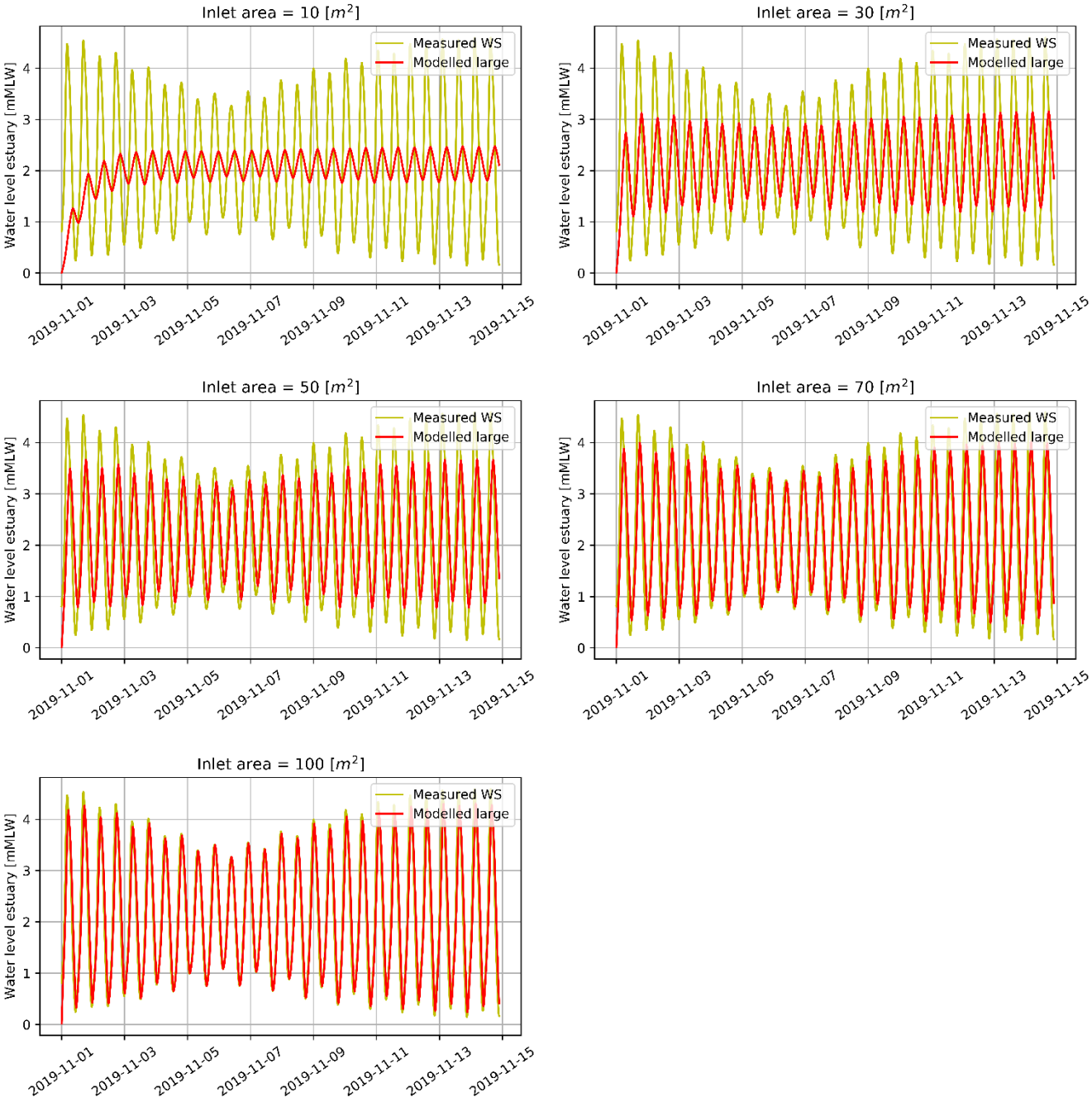

Figure A9 Modelled water levels in the polder and Western Scheldt for a normal tidal wave near Vlissingen. As input is the estuary water level measurements used from Vlissingen (Rijkswaterstaat, 2019). The solid yellow line indicates the measured water level in the Western Scheldt, water level relative to mean low water. The red dotted line indicates the modelled polder water level for a large polder with a varying inlet area. The tidal amplitude in the polders is reduced compared to the estuary. Further, the tidal amplitude in the polders depends on the size of the polder.

Appendix 12: Water levels for increased inlet areas

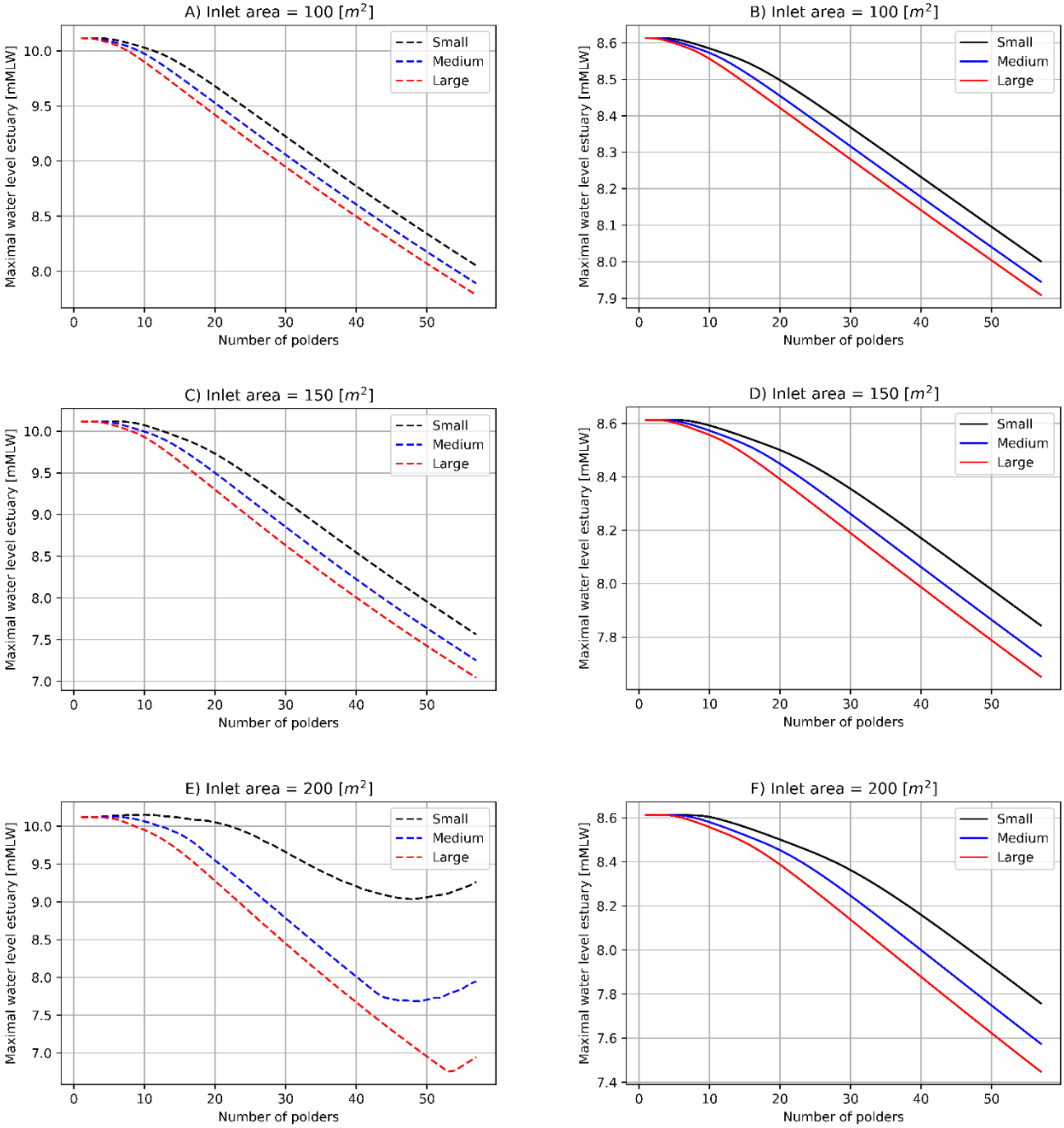

Figure A10 Maximal water level in the (solid) mid- and (dotted) upstream Western Scheldt, each line represents the water level in the Western Scheldt for 57 polders of a specific size. The optimal inlet area for upstream Western Scheldt polders is between 150-200m². The reduction in maximal estuary water level is lower for an inlet of 200m²(A10e) compared to smaller inlet areas. In the mid Western Scheldt is the reduction in estuary water level smaller, the optimal inlet area is beyond 200m².

Appendix 13: Effectiveness ratio

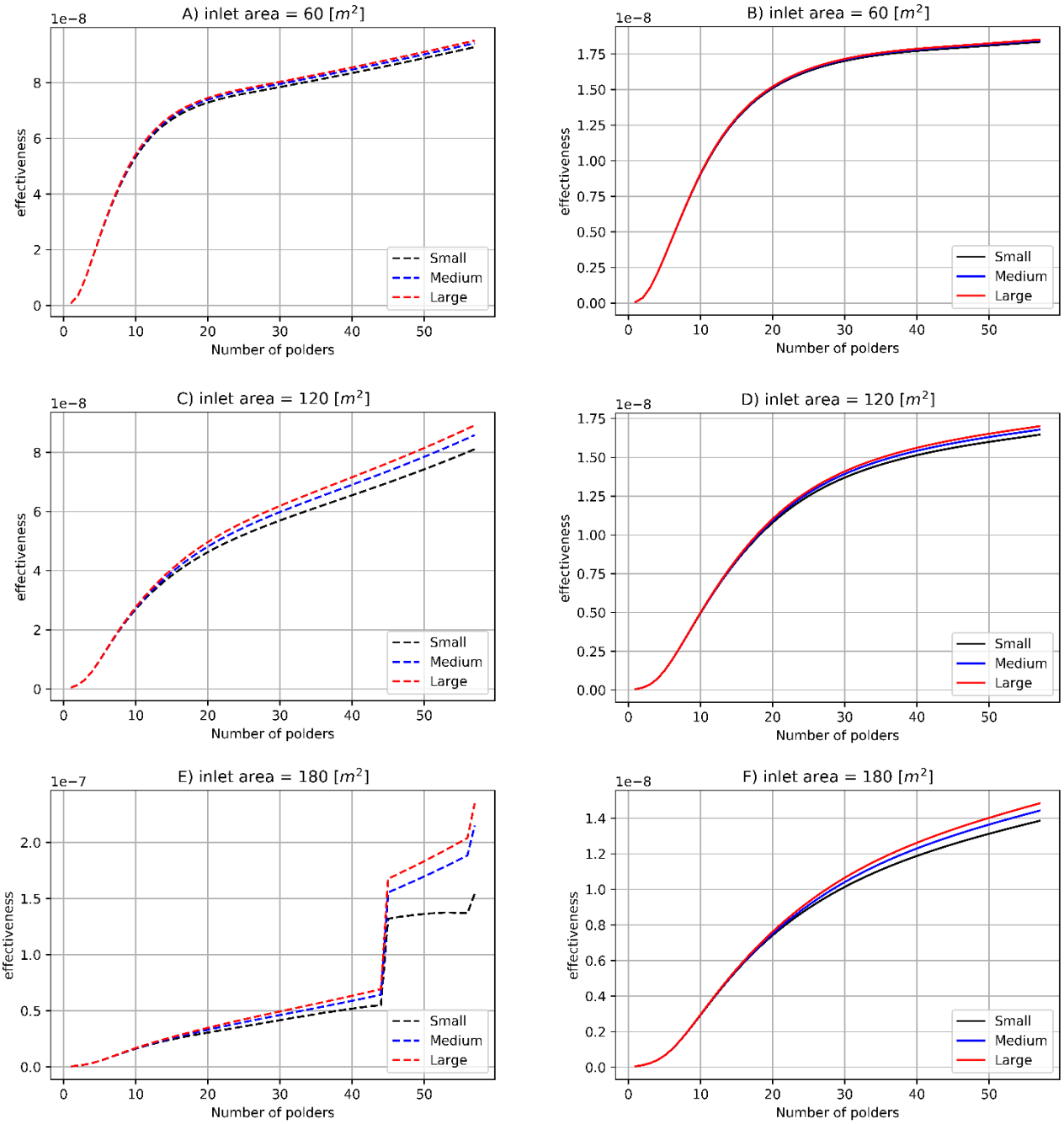

Figure A11 Effectiveness ratio calculated for simulations with varying inlet areas. Figures a,c and e are upstream in the estuary, b ,d & f are in the mi section of the estuary.

Appendix 14: CRT system

An alternative solution would be to apply a controlled reduced tide system (CRT), instead of the fully tidal exchanges system (FTE) like the current double dike in the model. A CRT has an inlet above mean high water (MHW) (Oosterlee et al., 2019) and an outlet at mean water level (MWL). During high water is the polder filled, however, in contrast to before can the polder only be emptied as the estuary water level is below mean water. The selected water levels are measured for Bath and Vlissingen, respectively the mid- and upstream section. The mean water levels are calculated over the period 01-11-19 until 01-12-19 to include a complete lunar cycle (M_2) (Neill & Hashemi, 2018), from Rijkswaterstaat (2019). The discharge equation in the script is rewritten with an if-statement, allowing inflow in the polder as the estuary water level (h_p) is above MHW and outflow when the estuary water level is below MWL (fig. A12).
The goal is to reduce the wave height during the storm surge and when it has passed, slowly release the stored water to the polder.

Location	MHW [mNAP]	MWL [mNAP]
Vlissingen	3.76	1.43
Bath	4.79	1.67

```
def discharge (h, hp):
    if h == hp:
        S = 0
        dis = 0
    else:
        S = (h-hp)/dw
        C = math.sqrt((8*g)/f)
        if S > 0 and h > MHW:
            u = C*(math.sqrt(dh*S))
            dis = u*inlet*60
        elif S < 0 and h < MWL:

            u = C*(math.sqrt(dh*S*-1))
            dis = u*inlet*60*-
        else:
            dis = 0
    return dis
```

Figure A12 discharge calculation in script, bold lines are the added if-statements for the CRT-system.

Calculating the water level for each size of polder with a varying inlet area shows similar results as the FTE double dike system (fig. A13-14) Next, the CRT system are tested with the ratio. As the previous results have indicated there is an optimal inlet area, so the ratios are calculated with the inlet area set to 100m^2. The results from figures A13-14, show no significant different results from the double dike system. In this model has the CRT system not lead to a further decrease in estuary water level, the argument to select a CRT over a double dike system is based on the reduced sedimentation with a CRT system (Jacobs et al., 2009; Maris et al., 2007; Oosterlee et al., 2019). If the estuary volume is smaller, than is the potential of a CRT system larger. This explains why CRT-systems are applied upstream along the Scheldt. A CRT-system provides no extra storm surge attention for the Dutch part of the Western Scheldt.

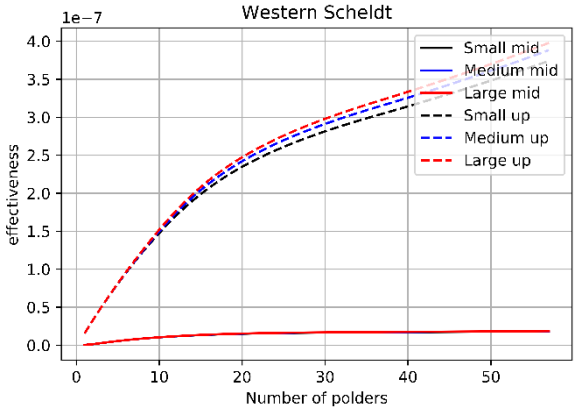

Figure A13 Effectiveness for the CRT-system in the midstream (mid) and upstream (up) section, inlet area = 100m^2

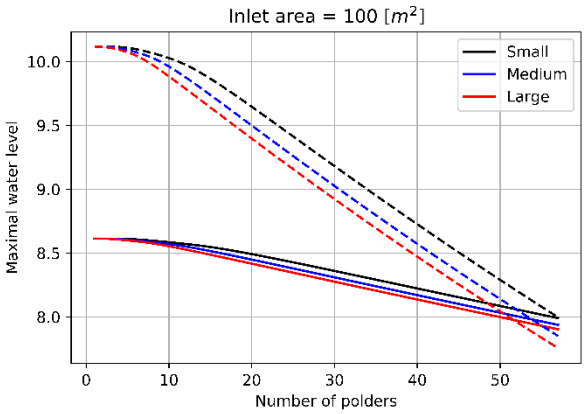

Figure A14 Water levels for the mid (solid) and upstream (dotted) Western Scheldt, inlet area is 100m2.

Appendix 15: Numerical error

When increasing the inlet area to large values (>200m^2) than- for specific polder sizes – happens something with the water level for the estuary in the model. See example in figure A18, a simulation of 28 small polders with an inlet area of 200m^2. I was not able to determine why this happened, but made sure than none of the other results in the report were influenced by this error. Thus, for certain simulations the model may give a wrong answer, however, this can easily be checked by plotting the Wester Scheldt water level curve. Therefore, I can say that this error has not influenced the results presented in this research.

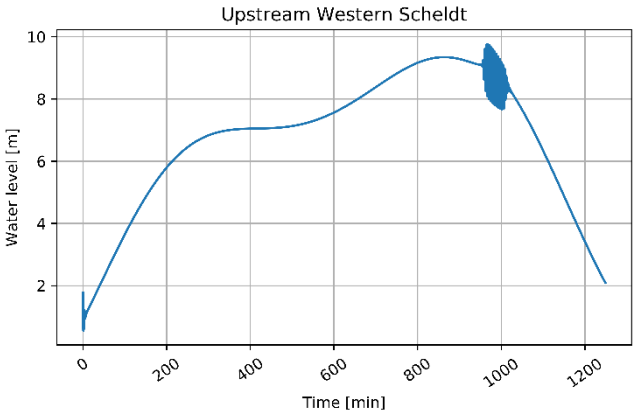

Figure A19 Example of error occurring with the Wester Scheldt water level, relative to mean low water.

Appendix 16: Electricity generation

The power (P) generated with a turbine can be estimated with equation A1, with the density of water (ρ), discharge (Q), gravity constant (g) and the head loss (Δh) (i.e. the difference in water level between estuary and the polder). The power is given in Watt, the discharge data in transformed in m^3/s and the head loss in meters.

[A1] $$P = \rho * Q * g * \Delta h = \rho * Q * g * (h - h_p)$$

As the difference in water level between the polder and in the estuary can be quite large, the potential for energy production is also large. However, a turbine has an efficiency around 80% (Nasir, 2013, 2014) and adding a turbine increases the friction. To understand what the total power output could the should the friction of the turbine be added to the model. The increased friction reduces the flow velocity through the inlet and thereby reduces the attenuation capacity. Further research should be done to understand the potential of the power generation in a double dike system.